CHARACTERIZATION OF HEAT TRANSFER IN NUTRIENT
MATERIALS WITH FORCED CONVECTION UTILIZING
CONVECTION OVEN DESIGN

A Thesis
Presented to
the Faculty of the Department of Mechanical Engineering
University of Houston

In Partial Fulfillment
of the Requirements for the Degree
Master of Science

---

by
Bal C. Trivedi
December 1976

CHARACTERIZATION OF HEAT TRANSFER IN NUTRIENT
MATERIALS WITH FORCED CONVECTION UTILIZING
CONVECTION OVEN DESIGN

An Abstract of
a Thesis
Presented to
the Faculty of the Department of Mechanical Engineering
University of Houston

In Partial Fulfillment
of the Requirements for the Degree
Master of Science

---

by
Bal C. Trivedi
December 1976

ABSTRACT

A heat characterization study for nutrient materials being processed in the convective oven of a space shuttle food system is presented. The study is limited to the case of foodstuffs stored in the cylindrical cans and thermostabilized to the ambient temperature of a space shuttle. A thermal model is developed to evaluate various methods of solution for the assumed configuration of the food heating process. It is observed that an explicit finite-difference solution is the most appropriate one due to (1) simplified computation, (2) ease of programming for a digital computer system, and (3) applications for parametric studies. A computer program is developed and its validity established by testing with known exact solutions. A parametric evaluation process is aimed at determining the effect of various parameters on the assumed "base" configuration. The analysis is used to determine "recommended" conditions for the food heating process. These conditions are derived by obtaining a balance between (1) the heating period and (2) the hot-spot and the cold-spot temperature differential in the food mass. Several temperature response charts are presented that establish the design guidelines. These charts provide a very practical tool to understand the effects of parameters like temperature of the heating medium, convection heat transfer coefficients at the boundaries of the can, thermal diffusivity of the substance, and aspect ratio of the food can on the heat transfer process.

TABLE OF CONTENTS

LIST OF FIGURES

LIST OF TABLES

NOMENCLATURE

A	area
Bi	Biot number
C_p	specific heat
Fo	Fourier modulus
h	convection heat transfer coefficient
k	internal conductance
L	length
m	divisions in a grid network
n	divisions in a grid network
r	radial coordinate
t	time period
T	temperature
z	axial coordinate
α	thermal diffusivity
α_o	thermal diffusivity of water
ρ	density
η	aspect ratio
θ	dimensionless temperature
Δ	small increment

Subscripts

a	ambient
avg	average value
c	cold-spot value
h	hot-spot value
i	evaluated at radial node i; also initial value

j	evaluated at axial node j
max	maximum value
min	minimum value
n	normalized
1,2,3	evaluated at surfaces 1,2,or 3 respectively
∞	heating medium

Superscripts

x	evaluated in the x-th time increment

1. INTRODUCTION

General

The food heating process in a space shuttle environment is different from the earth-bound facility for two important reasons: First, the zero-gravity situation precludes the convective mode of heat transfer through the food mass inside a container; and second, the limited amount of power available on a shuttle facility necessitates a highly efficient heating system.

For the present study, food is assumed an isotropic media which is stored and later processed in aluminum cans. These cans are sealed after pressurizing with nitrogen. During food heating in a space shuttle, it is heated to the desired serving temperature rapidly enough to prevent any significant growth of harmful bacteria.

Background

A previous study was designed to evaluate the heating process in a conduction tray for a Skylab configuration. Cylindrical containers of thermostabilized food were placed inside heated cavities. The heater is a constant thermal flux type which is turned off by a high-temperature switch when the can surface attains a specified high temperature. Thermal energy continues to diffuse by conduction inside the food mass during the off stage of the cycle. The can surface temperature falls to a specified value where a low-temperature switch turns the heater on and the heating phase repeats. Thus the tray provides a cyclic uniform heat flux that has a value zero (heater off) and a constant value (heater on) [3,7].

Cyclic Heat Flux Analysis. An analytical model was studied with the assumption of an infinite cylinder, heated along the cylindrical surface and insulated at the two ends [7]. A two-dimensional, transient heat conduction process under this assumption was analysed using known exact solutions. A digital computer was used to analyse and to verify the correctness of the thermal model. Temperature distribution in a mass of thermostabilized food material was obtained as a function of the radius of the can. While satisfactory results were obtained with the analytical model, it was decided not to apply it to the finite cylinder case for the following reasons [3]:

1. A discontinuity always exists when switching from one solution to the other due to the discontinuous manner in which the flux is switched on and off. The effect of this discontinuity is minor.

2. Considerable computation time is necessary and the time will increase considerably by the inclusion of the double summation required for the finite cylinder.

3. A finite-difference model appeared more attractive because of its reduced computation time and its versatility regarding different boundary conditions.

Finite-difference approach. This technique was utilized to carry out parametric investigations. Parametric studies involve the variation of each physical entity individually to establish the effect of that entity on the thermal response of the system. The computer program developed was used to study the effect of the power rating of the heater, the control temperatures which activate the heating element, the dimensions of the food can and the initial temperature of the food material. The results were presented in form of a series of temperature response charts [3].An optimum configuration was formulated by reviewing the results of the parametric studies as follows:

1, Heater power levels: Heating time can be significantly decreased by increasing the heater flux in the controlled heater upto about 0.5 Watts per square inch. Above that level, increasing the flux level simply inactivates the heater for longer periods of time and decreases the heating time only marginally. Hence, from the consideration of power utilization, the optimal condition would suggest a heater flux of around 0.5 Watts per square inch.

2. Control temperatures: The levels of the control temperatures have a significant effect on the heating time only when both the upper limiting value (T_{off}) and the lower limiting value (T_{on}) are increased simultaneously. Of particular interest is the fact that increasing the levels above 68.3°C (155°F) or decreasing the lower limiting value below 61.7°C (143°F) does not decrease the heating time signifi-

cantly.

3. Container size. It is necessary during the heating process to have the maximum heat transfer surface area per given volume of food. In the study to determine an optimum size, the height of the can is maintained at 1-1/8 inch while the radius is allowed to change. It can be seen that varying the can diameter on either side of the assumed value (3-3/4 inch) that the assumed value of the diameter is close to optimal.

The parametric values corresponding to a "recommended" status are repeated as follows:

Food can size:	Diameter	95 mm (3-3/4 inch)
	Length	28.5mm (1-1/8 inch)
Heater power levels:		0.5-2.0 watts per square inch
Control temperatures:	T_{on}	61.7°C (143°F)
	T_{off}	68.3°C (155°F)

<u>Food Heating System in a Space Shuttle</u>

In a study done for National Aeronautics and Space Administration, Fairchild Company stipulates a warming oven in which food packages are exposed to warm gases that pass over a tray with insert cavities for food containers [4]. A number of blowers are provided to maintain closed loop circulation. The gas becomes warm as it is swept past a number of thin foil resistance heaters. The gas gives up a large percentage of this heat to the food mass being heated. A small percentage is lost due to leakages from the oven.

Oven controls. The oven control methods may be selected to satisfy one or more of the following criteria:

1. A manually adjustable timer to cut off the oven heating following a set time period.

2. A high-temperature switch to cut off the oven heating to safeguard against burn out.

3. A high-temperature switch located in a tray insert to alarm a condition when a food package reaches the desired temperature.

Base configuration. The food shall be heated to attain an average temperature of 65^{0}C (149^{0}F). Moreover the total time the food stays under 140^{0}F shall be limited to 30 minutes since food decaying bacteria continue to grow under this temperature.

Thermal and Thermophysical Parameters. The values of parameters selected as a baseline estimate are presented as follows:

1. Convection heat transfer coefficients, in accordance with the Space Shuttle Food System Study by Fairchild are 22-33 Watts per sq. meter ^{0}C (4-6 Btu/hr ft^2 ^{0}F) [4].

2. Thermal diffusivity for most food materials is close to that of water. Besides, the reliability of published thermophysical properties is open to questions. Hence instead of using property values of nutrients, a dimensionless ratio called normalized diffusivity is used. Normalized diffusivity is the ratio α/α_0 where α is the thermal

diffusivity of the nutrient material and α_0 is the thermal diffusivity of water at standard temperature (5.3 cm^2/ hour). In accordance with the tables of thermophysical properties compiled by Cheng [2], chili with an upper limiting value of 5.63 cm^2/hour and tomatoes with a lower limiting value of 5.00 cm^2/hour constitute the extreme values of a narrow band of thermal diffusivity values for thermostabilized food.

3. Internal conductance. The internal conductance of foodstuffs has a large variation between foods. For the present analysis, internal conductance of water at the mid-point of the heating range is used. The heating range is 21°C to 65°C and its mid-point is 43°C. The associated internal conductance of water is 0.61 Watt/m °C.

4. Biot number. A Biot number of 2.0, being compatible with the assumed heat transfer coefficients, internal conductance and diameter of the food can, is considered for the present analysis.

2. FORMULATION OF THE PROBLEM

The heat transfer process is analysed by formulating a model following some simplifying assmptions. The model provides a technique to determine the temperature response following heating in a convective environment.

Mathematical Model

Basic assumptions. The simplifying assumptions follow:

1. Food substance stored inside the container has the shape of a circular cylinder which is concentric with its cylindrical container.

2. The heat transfer is through a mass of homogenous continuum in the shape of a finite cylinder. There are several limitations which may exist in a physical situation since the heat passes through a thin metal container and a layer of inert gases before it enters the mass of food. However, the error introduced due to the can metal will be insignificant since the metal container has very small thermal capacity and large internal conductance. This introduces a very small temperature gradient across the food can. The gap between the can and the food substance will have a very small internal conductance. In case the gap containing the gases is rather thin , the intergap temperature difference may be negligible.

3. An axisymmetric heat conduction takes place internal to the food material. This should be made possible by suitable convection oven design. This assumption makes it possible to analyze the present heating process as a two-dimensional heat transfer case in cylindrical coordinates.

4. A uniform convective heat transfer coefficient is present at the bottom, the top, and the cylindrical surface of the can. The coefficients may differ from one surface to another but is uniform at a surface. Any variations in the convective heat transfer coefficients in an actual case may be handled by obtaining average values across the surface.

5. A uniform free-stream temperature convective environment exists in the convection oven. The inherent oven design should be directed to achieve this objective.

Basic Equations

A cylinder with radius R and length L has an initial temperature T_i. It is placed in a medium of constant temperature T_a ($T_a > T_i$). The temperature distribution at a time t is given by

$$\frac{\partial^2 T}{\partial r^2} + \frac{1}{r}\frac{\partial T}{\partial r} + \frac{\partial^2 T}{\partial z^2} = \frac{1}{\alpha}\frac{\partial T}{\partial t} \tag{2-1}$$

where

$T = T(r,z,t)$;

$t>0$; $0<r<R$; $-L/2<z<L/2$

with initial condition

$$T(r,z,0) = T_i \tag{2-2}$$

and boundary conditions (see Figure 1).

$$\frac{\partial T}{\partial z} = -\frac{h_1}{k}\{T_a - T(r,-L/2,t)\} = 0 \tag{2-3}$$

$$\frac{\partial T}{\partial z} = \frac{h_2}{k}\{T_a - T(r,L/2,t)\} = 0 \tag{2-4}$$

$$\frac{\partial T}{\partial r} = \frac{h_3}{k}\{T_a - T(R,z,t)\} = 0 \tag{2-5}$$

Normalized Governing Equations

Characteristic dimensionless variables. A number of dimensionless variables are introduced to make the results of the study more versatile and to render the evaluation of parametric analysis more comprehensive.

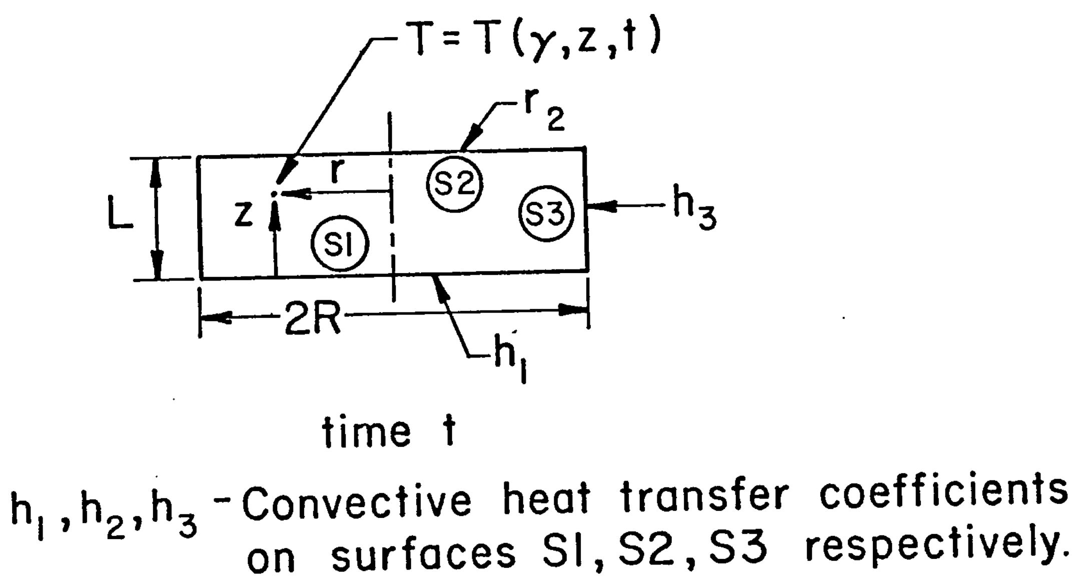

Figure 1 Cylindrical Mass of Food Material in a convective environment.

A list of dimensionless variables follows:

$\eta = L/R$, Aspect ratio

α/α_0, Normalized thermal diffusivity

$\Theta=(T-T_i)/(T_a-T_i)$, Dimensionless temperature

$Fo=\alpha t/R^2$, Dimensionless time

$Bi_1=h_1R/k$, $Bi_2= h_2L/(2k)$, $Bi_3=h_3L/(2k)$.

Fo is the Fourier Modulus and Bi is the Biot number.

Normalized equations. Substituting these dimensionless variables in the governing equations (2-1) to (2-5) and simplifying, it can be shown that

$$\frac{\partial^2\Theta}{\partial r_n^2} + \frac{1}{r_n}\frac{\partial\Theta}{\partial r_n} + \frac{\partial^2\Theta}{\partial z_n^2} = \frac{\partial\Theta}{\partial Fo} \tag{2-6}$$

where

$$\Theta = \Theta(r_n,z_n,Fo);\ Fo>0;\ 0<r_n<1;\ -.5\eta<z_n<.5\eta.$$

with initial condition

$$\Theta(r_n,\ z_n,0) = 0 \tag{2-7}$$

and boundary conditions

$$\frac{\partial\Theta}{\partial z_n}=Bi_1\{\Theta(r_n,0.5\eta,Fo)-1\} \tag{2-8}$$

$$\frac{\partial\Theta}{\partial z_n} = -Bi_1\{\Theta(r_n,-0.5\eta,Fo)-1\} \tag{2-9}$$

$$\frac{\partial\Theta}{\partial r_n} = -Bi_1\{\Theta(1,z_n,Fo)-1\} \tag{2-10}$$

where

$r_n = r/R$; $z_n = z/R$;

$\Theta_a = (T_a-T_i)/(T_a-T_i)=1$; $\Theta i=(T_i-T_i)/(T_a-T_i)=0$.

It should be observed here that the normalized form of governing equations are free of terms involving the size of the container, the thermal diffusivity of food and convection heat transfer coefficients of the heating medium. Moreover the initial temperature of the food material is normalized to zero and the temperature of the convective medium is normalized to 1. Hence the solution for these equations will have generalized applications in all problems of a similar class.

Physical significance of the dimensionless numbers. The Biot number written as $Bi = h/(k/r)$ can be interpreted as the ratio of surface to internal thermal conductance. A high Biot number makes the temperature at the boundary of the cylinder approach the temperature of the convective environment. Hence, the case of heat transfer with constant surface temperature is a special case of the present formulation.

Another case of practical significance is present when the Biot number is extremely small. This happens when $k \to \infty$ or when $h \to 0$. In either case the Biot number approaches a limiting value of zero. Under these circumstances the temperature gradients at the boundary surfaces are extremely small. The heat transfer process, as before, is a special case of the present formulation.

3. ANALYTICAL TECHNIQUES

Analytical methods are most appropriate when an exact solution to a heat transfer problem is desired. Solutions known in available literature in heat transfer are reviewed for the purpose of ascertaining their applicability to the present case of heat characterization.

Theory of Generalized Variables

A dimensionless number can be formed by suitable grouping of a number of variables in the form of an expression. Such a dimensionless number has a physical significance and is called a generalized variable. The Fourier Modulus, the Biot number, the aspect ratio, and the dimensionless temperature defined earlier are all examples of such variables.

Problems of heat transfer can be formulated by using individual variables representing geometry and thermophysical properties of the substance being heated and properties of the heating medium. The resulting equations will involve a large number of independent variables. A change in any of these variables will require that the solution to the set of equations be repeated afresh. Thus the applicability of the solutions obtained in this manner is rather limited.

A preferred approach is to use dimensionless numbers.

To illustrate the point, a formulation using Fourier Modulus eliminates terms involving time , density of the heated substance, specific heat of the heated substance, its internal conductance, and characteristic length. The solution obtained in this manner will have immediate applications even when one or more of these variables change. Further examples of generalized variables are shown in Table 1.

Table 1. Generalized Variables

Generalized Variables	Individual Variables
Fourier Modulus, Fo	time, t density, ρ specific heat, C_p internal conductance, k
Biot number, Bi	convection heat transfer coefficient, h radius, r internal conductance, k
Aspect ratio, η	length, L radius, r
Temperature, Θ	dimensioned temperature, T temperature of the heating medium, T_∞ initial temperature, T_i

Basic Analytical Techniques

A linear, homogenous partial differential equation of heat conduction along with the equations of relevant boundary conditions and of initial condition represent a boundary-value problem. In literature on mathematical physics, analytical methods of solution for specific problems in heat conduction are available.

Three basic analytical techniques and their applicability to the present study are presented in Appendix A. A summary of the results is as follows:

1. Solution by Separation of Variables. The temperature transient as derived in Appendix A is given by

$$\Theta(r_n, z_n, Fo) = \sum_{i=1}^{\infty} \sum_{j=1}^{\infty} A_i\, B_j\, Jo(\beta_i\, r_n).\cos(\mu_j\, z_n).\exp\{\beta_i^{\,2} + \mu_j^{\,2})Fo\} \qquad (A-5)$$

where

$$A_i = \frac{2Bi_3}{Jo(\beta_i)(\beta_i^{\,2} + Bi_3^{\,2})} ;$$

$$B_j = (-1)^{j+1} . \frac{2Bi_1(Bi_1^{\,2} + \mu_j^{\,2})^{0.5}}{\mu_j(Bi_1^{\,2} + Bi_1 + \mu_j^{\,2})}$$

The solution obtained in this form has the following limitations:

a) A double summation series needs a large computation time.

b) The eigen values, β_i and μ_j, have to be derived from the characteristic equation and that involves additional computation.

c)The convection heat transfer coefficients at the two faces of the can are assumed to be equal.

2. Solution by Operational Methods. The classical methods of separation of variables is not applicable to a set of non-homogenous differential equations and hence cannot be applied to the case involving generation of heat. An operational technique is the next choice. Three distinct types of operational methods are: (1) Laplace Transform, (2) Fourier Transform and (3) Hankel Transform. Appendix A shows the details of these methods.

These methods are limited to problems in infinite regions. The Laplace Transform is individually applied to the case of an infinite plate and an infinite cylinder. A finite cylinder case is obtained by superposition of these two solutions. The solution has the same limitations as in the case of solution by Separation of Variables.

3. Solution by Finite Integral Transform Method. This method can be directly applicable to the heat transfer problems in a finite region. Olcer developed a generalized solution to a class of heat flow problems in a finite cylinder. The solution for a three-dimensional, unsteady heating of a finite, solid circular cylinder exposed to heating in a convective environment has been discussed in the cited reference [8].A special case showing axisymmetric heat flow and uniform initial temperature is presented in Appendix A.

It should become clear from the solutions in the Appendix that the technique of Finite Integral Transform Method results in complex expression for the temperature distribution and will require large computation time. Hence in spite of the capability of this method, its practical application to the present heat characterization study is not recommended.

Concluding Remarks

All the methods reviewed so far have the limitations of (1) complexity, (2) large computation time and (3) lack of versatility. The parametric evaluation, a very important tool in a heat characterization study, is not possible under these conditions. Next, the numerical approach is considered as an alternative.

4. NUMERICAL TECHNIQUES

Numerical techniques can be classified as (1) those requiring nodal or element description on, and within, the boundary of domain of interest and (2) those requiring description only on the boundary of the domain. The first class consists of finite-difference and finite-element methods. The second classification includes those methods generally described as collocation methods and includes many different techniques. "Point-matching" and singular integral techniques are forms of the boudary collocation approach. They are generally suitable for steady-state heat conduction problems [9]. Hence the boundary collocation techniques, despite being highly accurate and computationally efficient are not suitable for transient heat conduction problems.

Finite-Difference Techniques

At present the finite-difference method is an efficient one for the approximate solutions for heat conduction problems, both transient and steady-state cases. It is based on the replacement of the derivatives by their finite-difference equivalents. As a result of such transformations, the differential equation of heat flow is replaced by an equivalent algebraic equation. Evidently, the solution of these algebraic equations is easy and gives accurate results.

The region to be analyzed (a finite cylindrical mass of food material) is made up of small but finite elements, as shown in Figure 2.

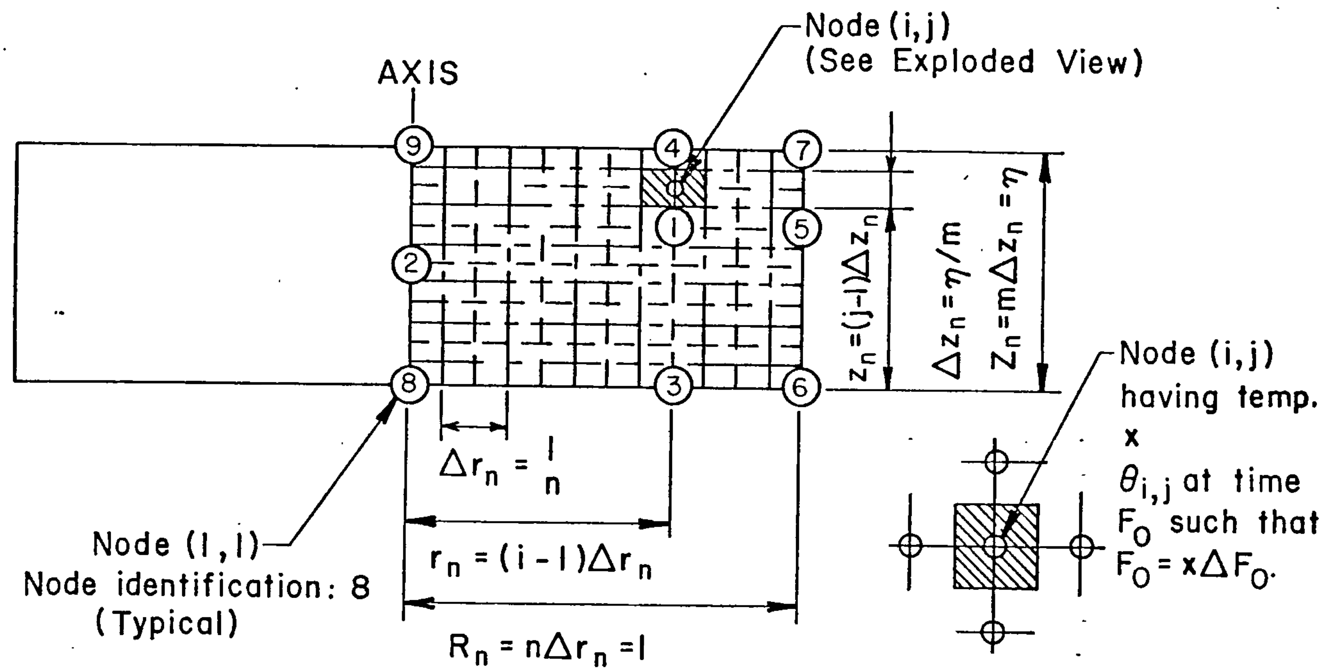

Figure 2. Grid Network for a Cylinder having Normalized Dimensions $R_n = 1$, $Z_n = \eta$.

The network consists of a grid m by n where a section of the cylinder is divided into m equal parts along the axis and n equal parts along the radius. By the assumption of axisymmetry, no temperature variation exists in different angular positions within the cylindrical mass. Each internal finite element has a width Δr and a height Δz given as

$$\Delta r = R/n, \; \Delta z = \eta R/m;$$

or in dimensionless form,

$$\Delta r_n = 1/n, \; \Delta z_n = \eta/m.$$

The centroid of each finite element, called a node, is given the grid coordinates (i,j). The node number 8 is at the center of the grid coordinate system and is assigned coordinates (1,1). The position coordinates and the grid coordinates have the relationship given as

$$r_n = (i-1)\Delta r_n, \quad z_n = (j-1)\Delta z_n.$$

The temperature of a node is the average temperature of the associated finite element and at time t is addressed as $\Theta^x_{i,j}$ where

$$Fo = x.\Delta Fo = x.(\alpha\Delta t/R^2) = \alpha t/R^2$$

The nodal system is classified in two groups: internal nodes and boundary nodes. An internal node belongs to a finite element that is separated from all boundary surfaces by at least one intervening finite element. In Figure 2, nodes number 1 and 2 are examples of internal nodes. Nodes number 3 to 9 are boundary nodes.

Explicit and Implicit Finite-Difference Techniques

The finite-difference equations for the temperature response at different node points are given as follows:

Explicit formulation. Different equations are obtained for an internal node as compared to a boundary node.

$$\text{internal node: } \Theta^{x+1}_{i,j} = \Phi(\Theta^x_{i,j}, \Theta^x_{i\pm1,j}, \Theta^x_{i,j\pm1}) \qquad (4\text{-}1)$$

$$\text{boundary node: } \Theta^{x+1}_{i,j} = \Phi(\Theta^x_{i,j}, \Theta^x_{i\pm1,j}, \Theta^x_{i,j\pm1}, \chi) \qquad (4\text{-}2)$$

where Φ is a functional relationship and χ is a term that introduces the effect of boundary conditions in the relationship shown here.

Implicit formulation. The relationship showing the temperature response of internal and boundary nodes can be expressed as follows:

$$\text{internal node: } (\theta^{x+1}_{i,j},\ \theta^{x+1}_{i\pm1,j},\ \theta^{x+1}_{i,j\pm1}) \doteq \Phi(\theta^{x}_{i,j}) \quad (4\text{-}3)$$

$$\text{boundary node: } (\theta^{x+1}_{i,j},\ \theta^{x+1}_{i\pm1,j},\ \theta^{x+1}_{i,j\pm1},\chi) = \Phi(\theta^{x}_{i,j}) \quad (4\text{-}4)$$

It should be noted that some of the terms shown above may not be influential for boundary nodes.Implicit finite-difference technique provides the future temperature of different nodes in terms of the present temperature at a specific node. One may have to solve a number of simultaneous equations in order to determine the future temperature at the specific node in reference. Thus the computation gets involved. The merit of an implicit technique lies in its unconditional stability.

Explicit finite-difference technique, in contrast, provides the future temperature at a specific node in terms of the present temperatures at a number of nodes surrounding it. The solution of a single equation gives the results showing the future temperature at a specific node. Consequently, the computation is simpler as compared to the implicit technique. The explicit model may become unstable if the time increments selected for the iteration process are not adequately small. In certain situations the time increments may have to be decreased to an extent that increased computation time may offset the advantage of simplicity.

Appendix B shows the detailed analysis of the finite-difference equations that converts the set of explicit equations in a form that lends itself to analysis and computation on a digital computer. The analysis is centered on an iteration process that calculates the temperature distribution within the food substance, given the initial and boundary conditions.

Computation

Appendix C shows the flow chart, a listing of the computer program and a typical output result obtained as a result of computer analysis.

5. TESTING OF FINITE-DIFFERENCE FORMULATION

In order to verify numerical procedures; it is desirable to consider limiting cases especially when exact solution or experimental evidence is available for such cases. Exact solutions are available in the literature for (1) an infinite cylinder, (2) an infinite plate and (3) a short cylinder. Appendix C shows the comparisons between the solutions derived on a digital computer based on explicit finite-difference technique and the ones basically obtained from available exact analytical techniques.

Limiting cases

Infinite cylinder. The results of the numerical analysis are obtained for a long cylinder having an aspect ratio of 10.8. The internal conductance is assumed very large, and the thermal diffusivity is assumed to be ten times that of water. Figure 3 shows the temperature response along the axis of the food mass (Θ_c) and Figure 4 shows the temperature response at the surface of food mass (Θ_s). These figures also show the exact solutions taken from the temperature response charts drawn by Schneider . These charts are for an infinite cylinder with infinite internal conductance [11]. The close correlation between the numerical and the exact solutions is a proof of validity of the finite-

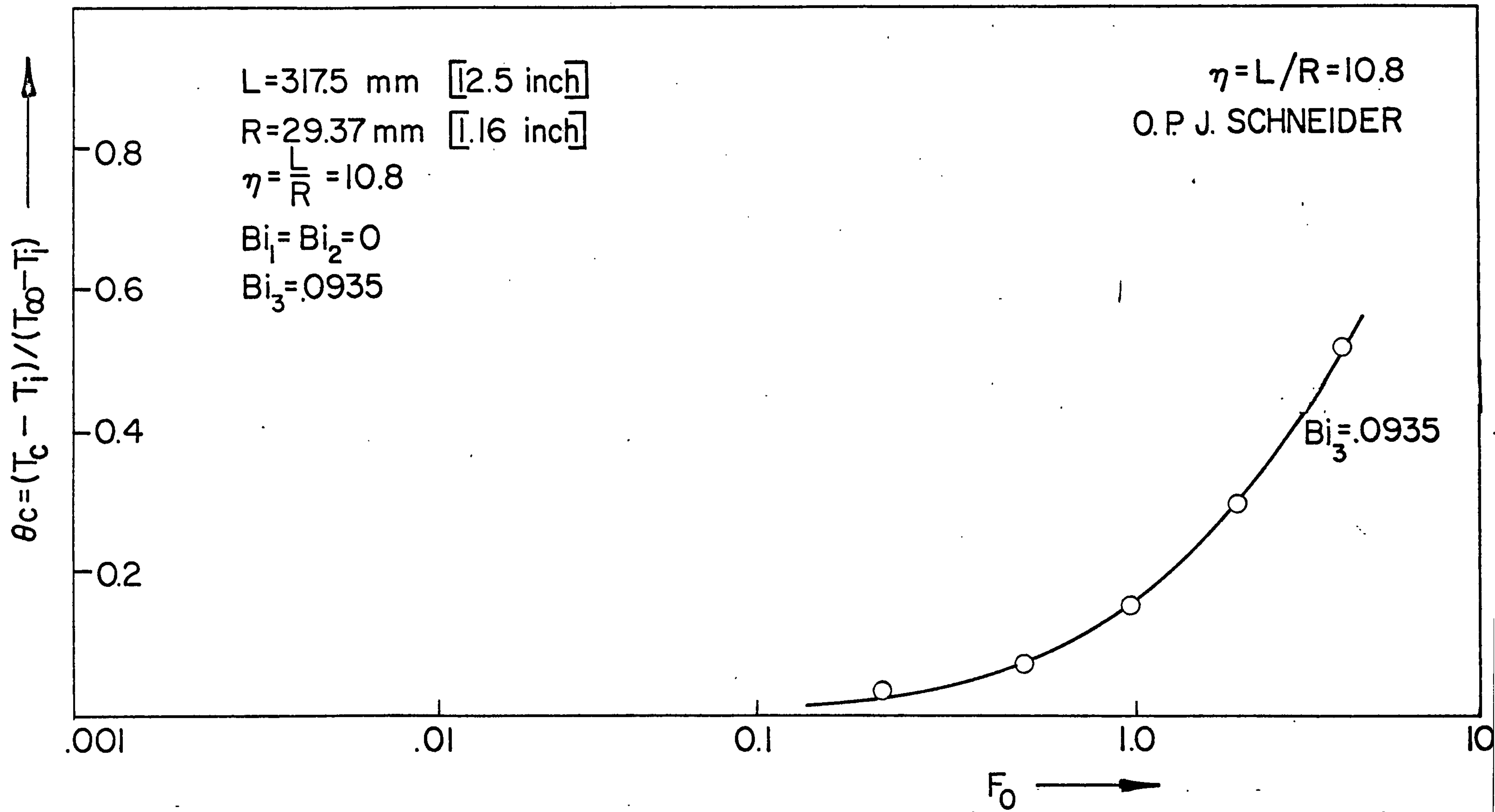

Figure 3 Axial Temperature Response for an Infinite Cylinder with Infinite Internal Conductance.

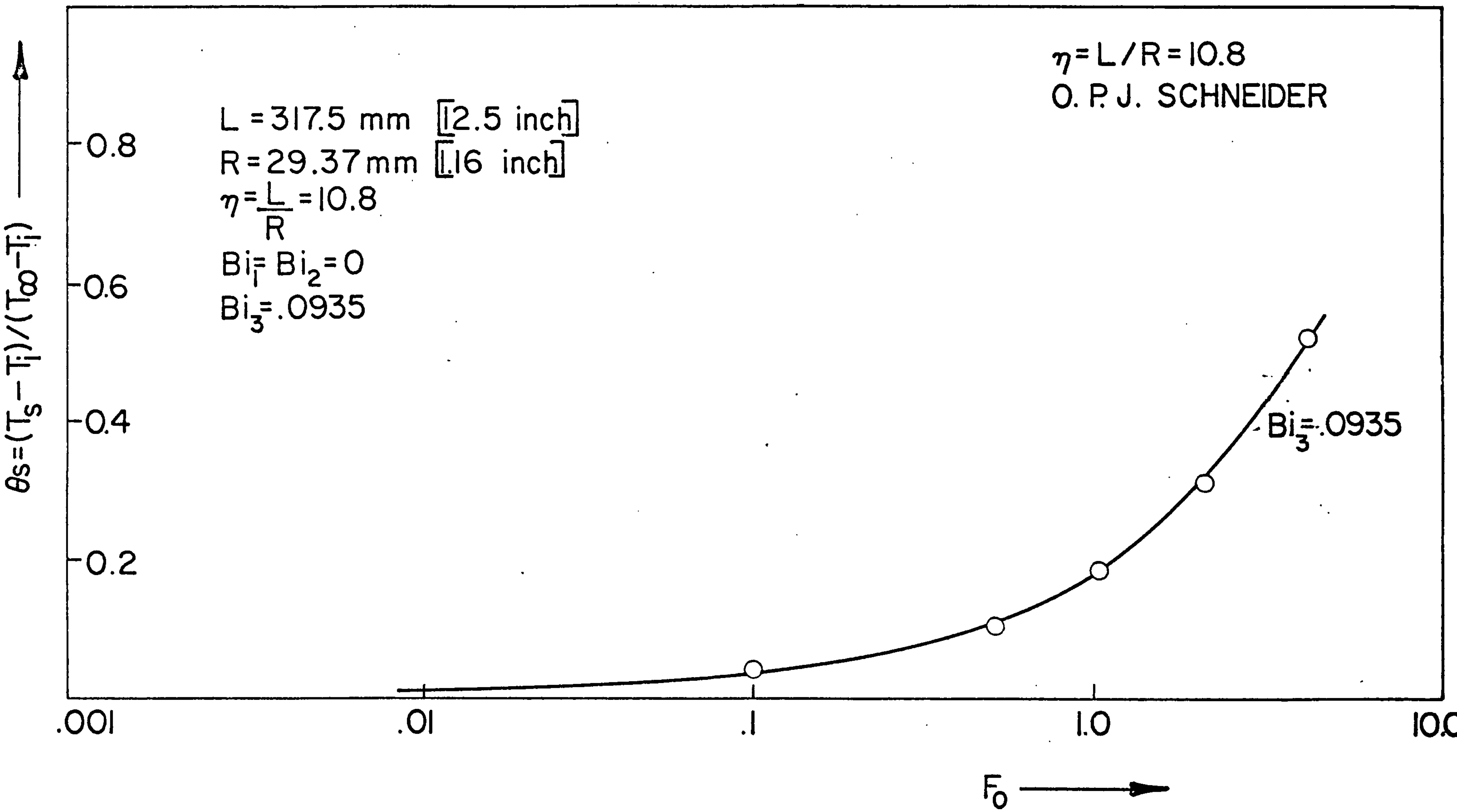

Figure 4. Surface Temperature Response for an Infinite Cylinder with Infinite Internal Conductance.

difference formulation.

Short cylinder. The numerical solution presented in Figure 5 was based on assuming a very large internal conductance, reflected in a thermal diffusivity value which was ten times that of water. An aspect ratio of 2 was also assumed. These results are compared with exact solutions available in the form of temperature charts by Schneider. The charts were based on assuming an infinite conductance and an aspect ratio of 2. The close correlation evident from the Figure 5 is a further proof of the present formulation.

Case of a Finite Cylinder

Product solutions techniques. The technique as explained in Appendix D uses solutions available for an infinite cylinder and an infinite plate to obtain the temperature response in a finite cylinder. By various combinations of infinite plate thickness and radius of the infinite cylinder, all sizes of the finite cylinder can be modeled. Since exact solutions of the infinite cylinder and the infinite plate are available [6,11], the product solution technique is applied to obtain the temperature response in case of cylinder having an aspect ratio of 1.0 and 2.0 respectively. Figures 6 and 7 show the comparison between the numerical solutions obtained by the finite-difference formulation and the results computed by product solutions method. The temperature response is expressed as

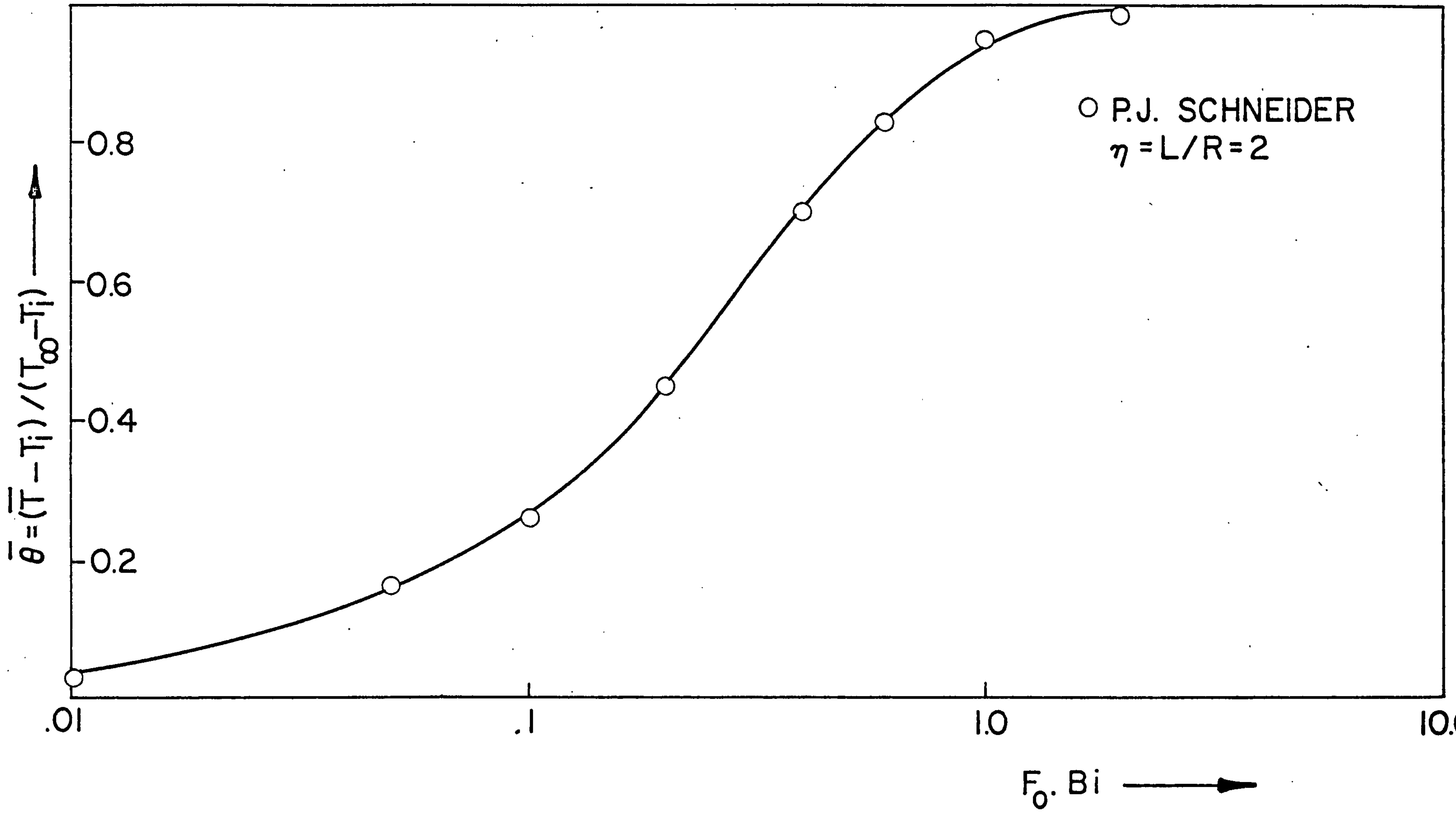

Figure 5 Temperature Response in a Short Cylinder with Infinite Internal Conductance.

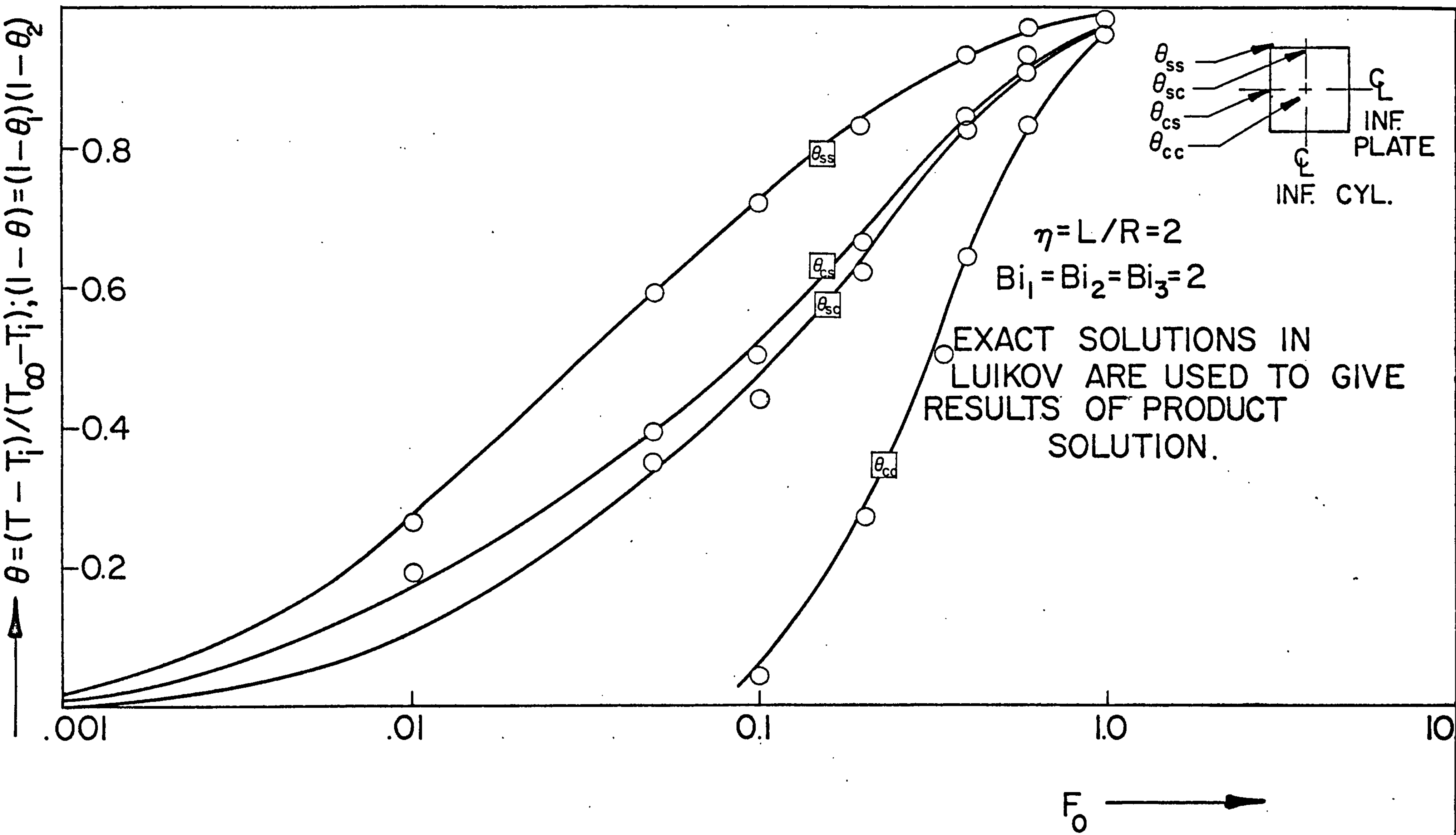

Figure 6 Temperature Response in a Short Cylinder

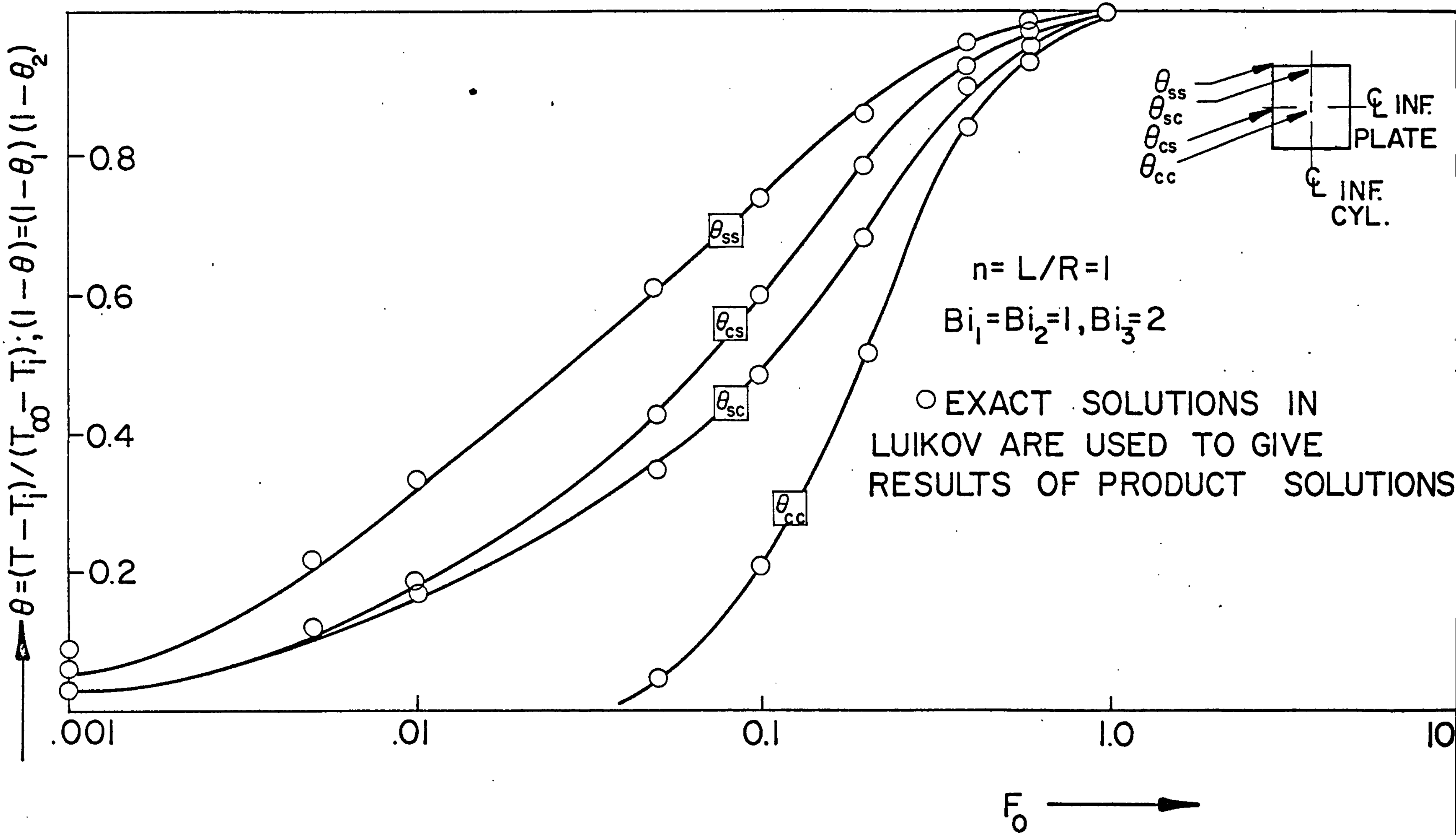

Figure 7 Temperature Response in a Cylinder having aspect ratio of 1.0

$$(1-\theta) = (1-\theta_1).(1-\theta_2)$$

where

θ is the temperature in the food mass,

θ_1 is the temperature in the infinite plate, and

θ_2 is the temperature in the infinite cylinder.

All the temperatures are taken for a specific point in the medium being heated at a specified time. The close correlation obtained and shown in Figures 6 and 7 is a further proof of the validity of the present formulation.

Discussion

The comparisons of the previous sections show that the results obtained by numerical analyses are in general agreement with the exact solutions. The results are valid in the limiting cases just discussed and in the general case of a finite cylinder. In the following sections, the numerical technique validated here is used to study the effect of variable parameters on the heating period and on the temperature distribution within the mass of food.

6. PARAMETRIC STUDIES

Several numerical solutions, as listed in Appendix C , are obtained for the purpose of heat characterization study and parametric investigation in the food heating system. A number of temperature response charts are plotted following these case runs to gain insight into the heating system.

Temperature Response Charts

Temperature response charts are grouped in two separate classes as evidenced by Table 2. The first class of charts shows the pattern of temperature variation with respect to Biot numbers; while the aspect ratio is held constant. This class of charts is shown on a semi-logarithmic scale in Figure 8. The second class of charts, shown in Figure 9, shows the pattern of temperature variation with respect to aspect ratio when the Biot number is held constant. The dimensionless temperature is the dependent variable and the dimensionless time or the Fourier Modulus is the independent variable. The semi-logarithmic scale gives "S" shaped curves that present a better resolution for the temperature variable and provide reasonable accuracy on the upper end of the temperature scale.

Table 2. Classification of Temperature Charts

Class of Charts	Constant Parameter Values	Variable Parameter Values	Reference Figure Number
1	η	Bi_3 varies 0.1 to 20	
	0.4		8(a)
	0.6		8(b)
	0.8		8(c)
	1.08		8(d)
	1.4		8(e)
	2.0		8(f)
	6.0		8(g)
	10.0		8(h)
2	Bi_3	η varies 0.4 to 10	9

The response charts are used to study the effect of changes in parameters such as (1) the temperature of the heating medium, (2) the convection heat transfer coefficient on each surface, (3) the thermal diffusivity of food mass, and (4) the aspect ratio of the cylindrical mass when the volume is fixed.The study determines the effect on heating period and on the differential between the hot-spot and the cold-spot temperatures in food substance.

The values of dimensionless time and temperature are obtained from the temperature response charts , Figures 8 and 9, by interpolation if necessary. These variables are converted back into dimensioned quantities.

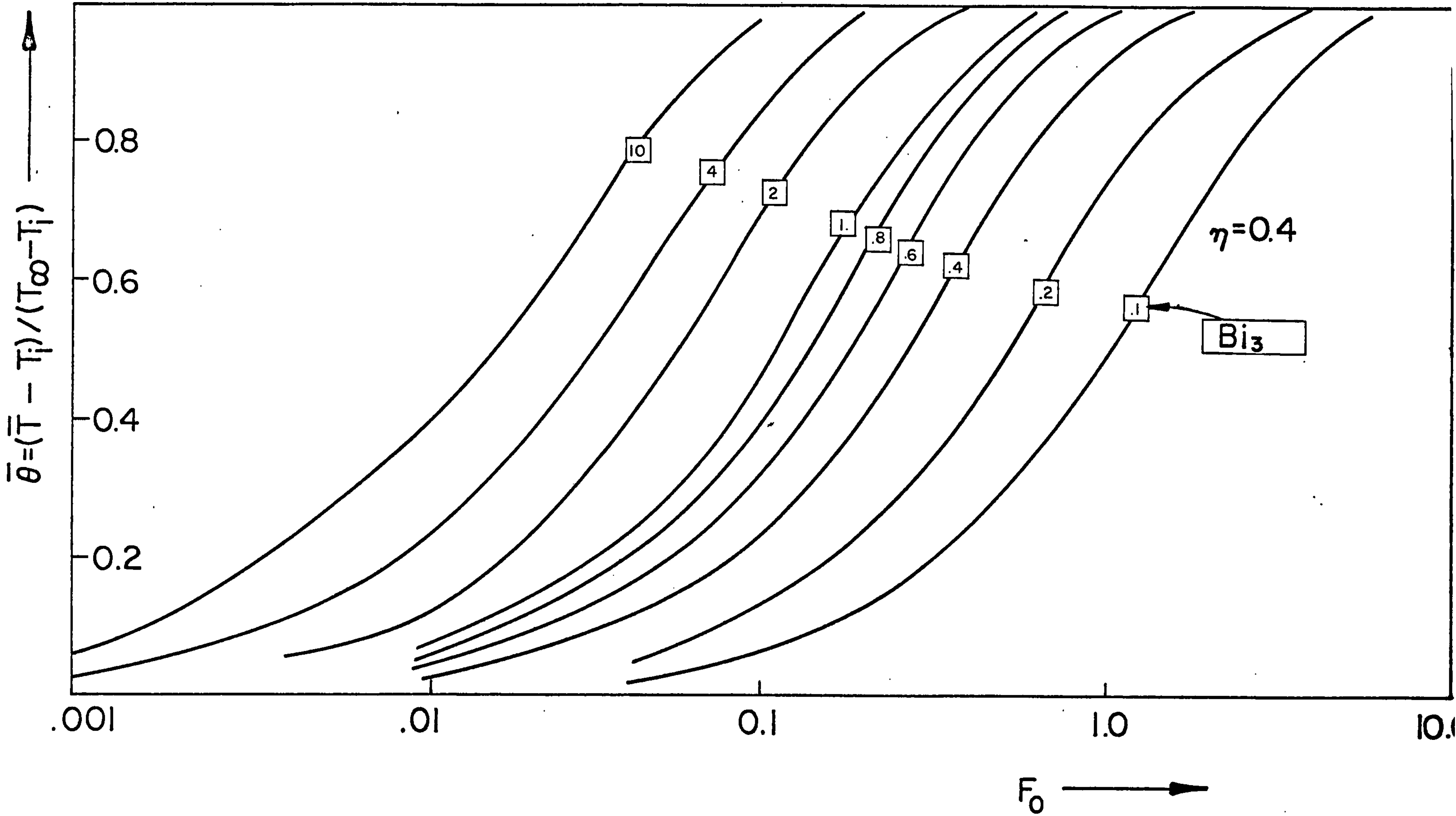

Figure 8 Temperature Response for a Finite Cylinder in a Convective Environment: (Fixed Aspect Ratio)
(a) $\eta = 0.4$

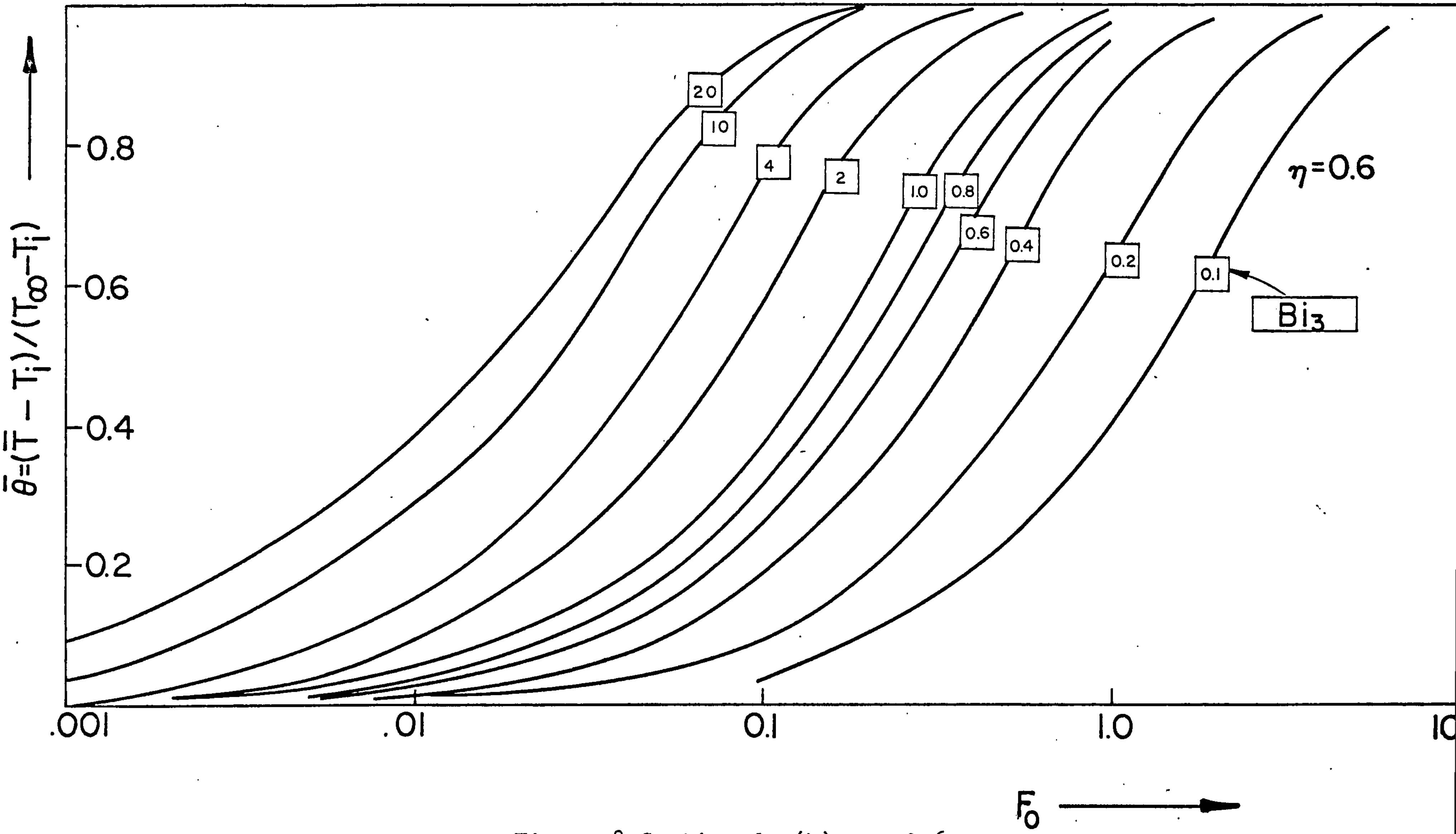

Figure 8 Continued; (b) η = 0.6

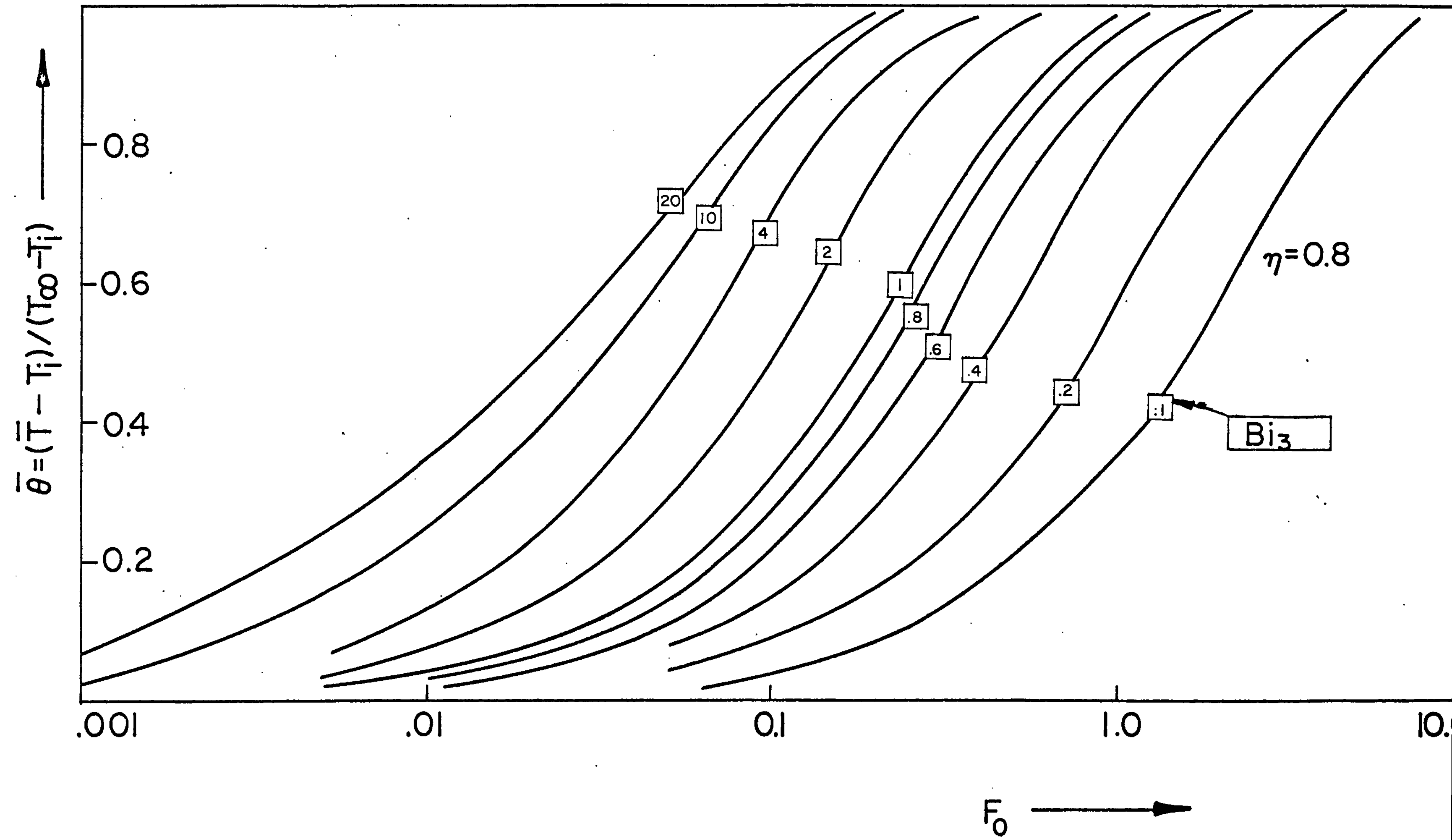

Figure 8 Continued; (c) η = 0.8

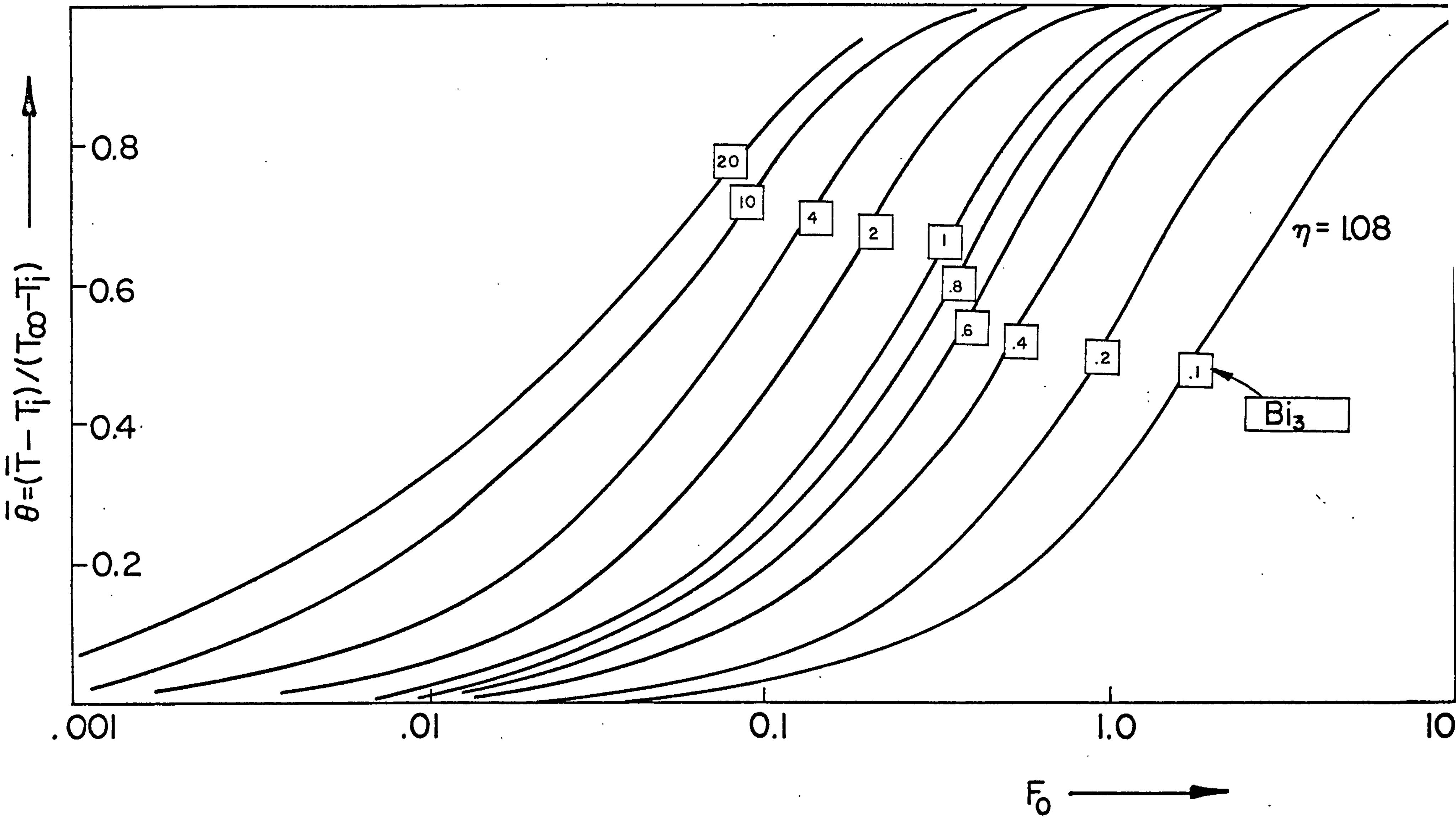

Figure 8 Continued; (d) η = 1.08

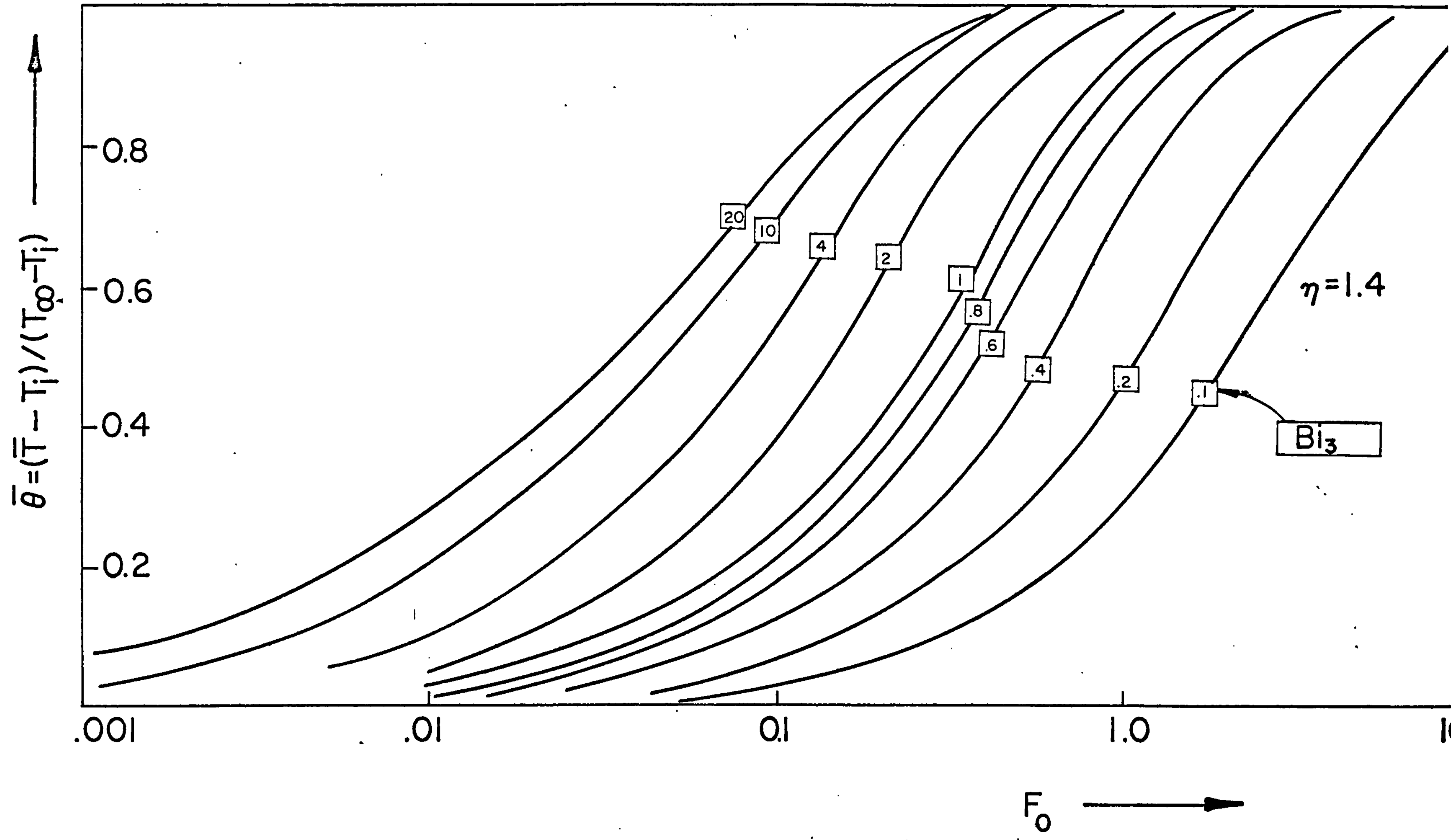

Figure 8 Continued; (e) η = 1.4

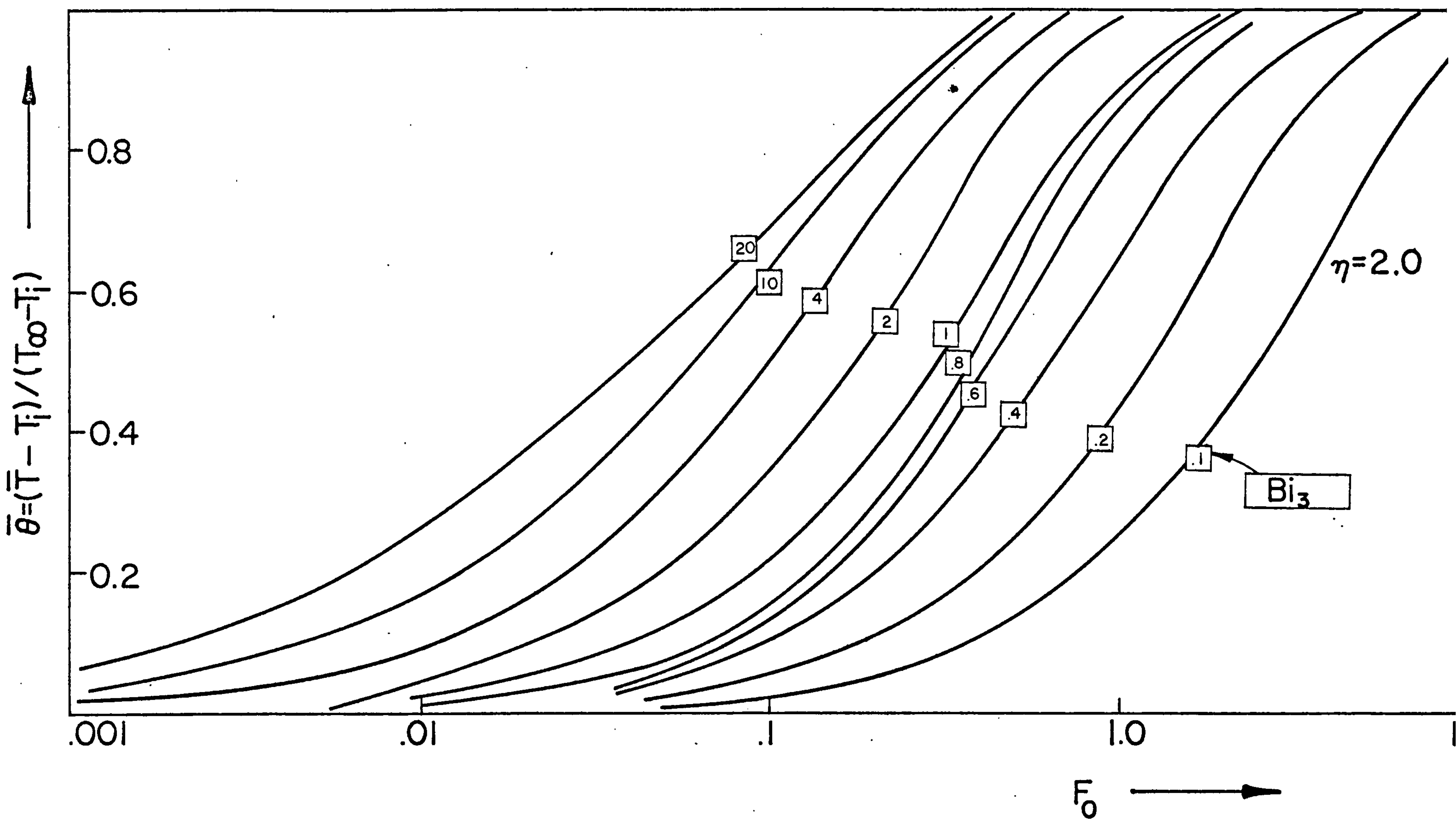

Figure 8 Continued (f) η = 2.0

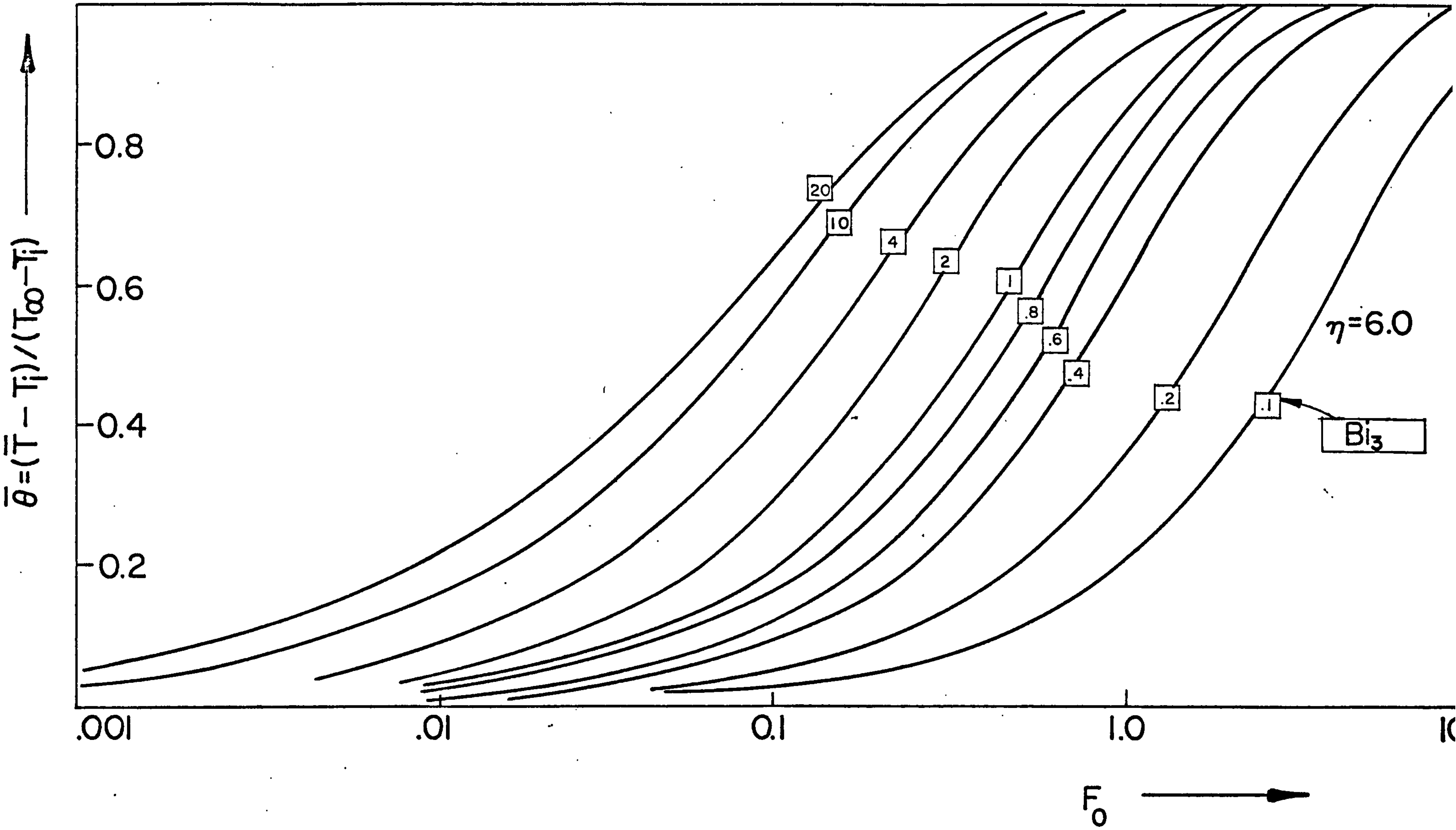

Figure 8 Continued; (g) η = 6.0

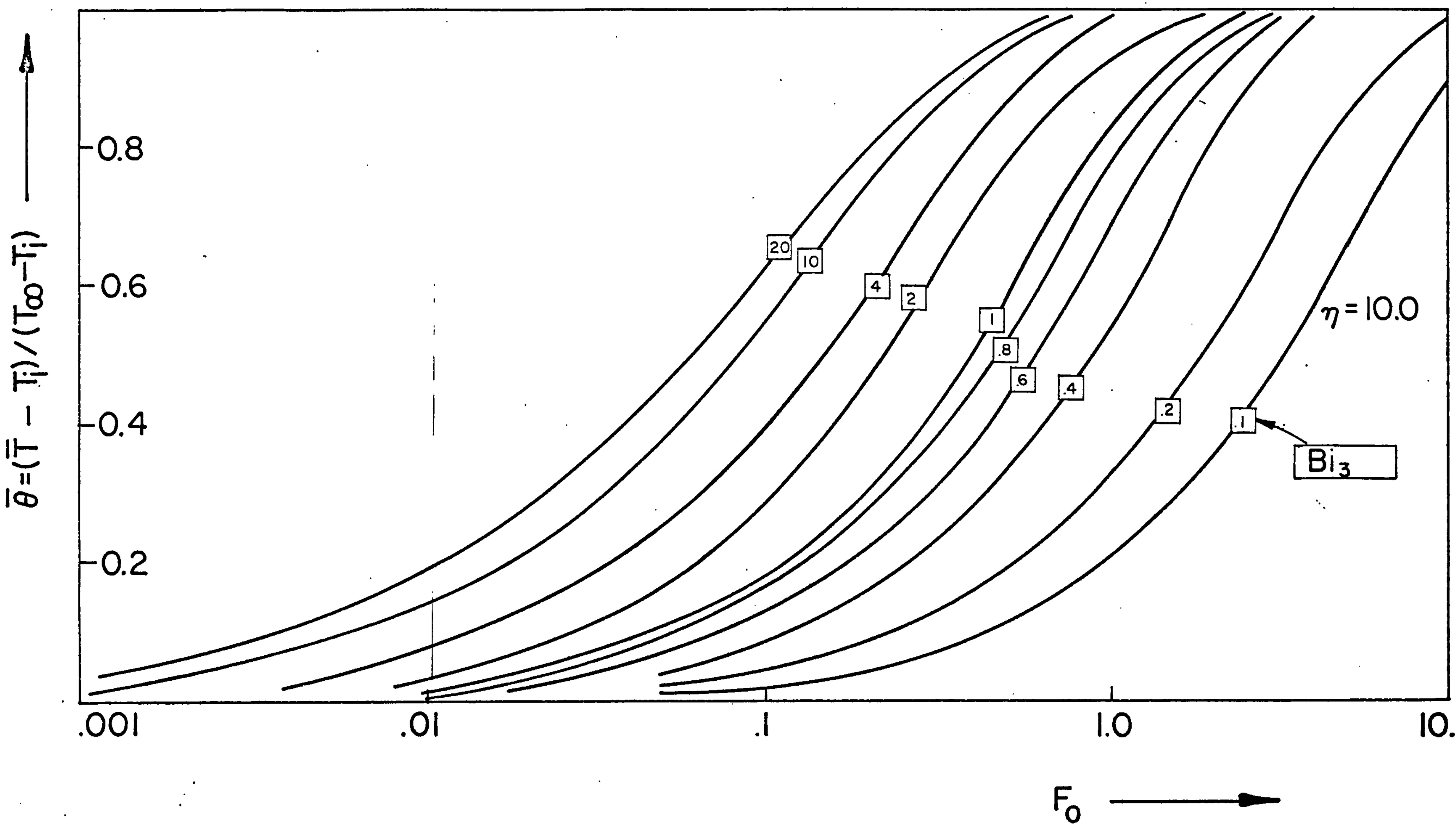

Figure 8 Continued; (h) η = 10.0

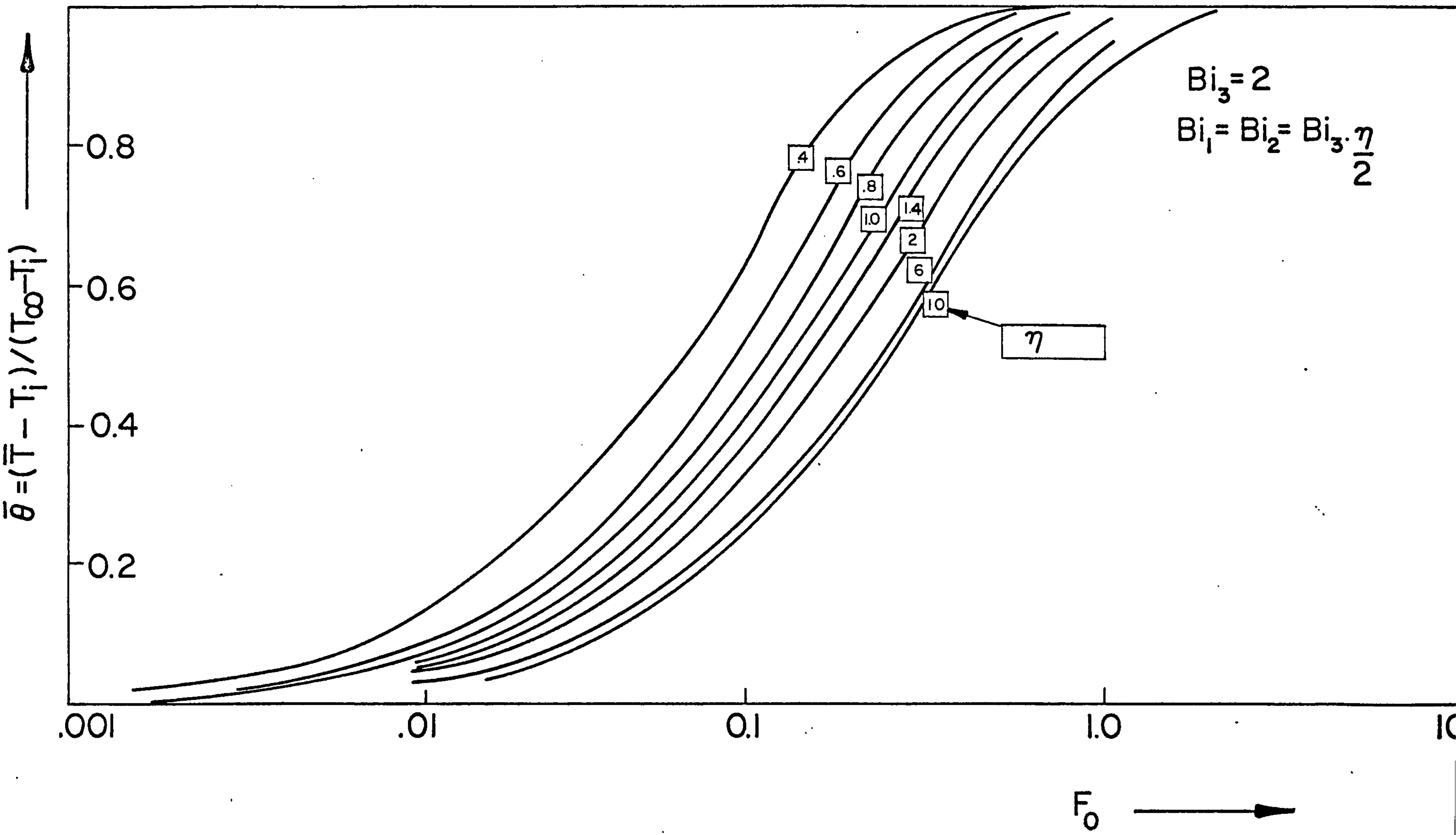

Figure 9 Temperature Response for a Finite Cylinder in a Convective Environment: Bi is Fixed

Parametric Studies

Basic configuration. The parametric studies are centered around a base configuration developed with the assumptions in the earlier stated guidelines. The food can size is to be 95 millimeter (3-3/4 inch) diameter, 28.5 millimeter (1-1/8 inch) long with 204 cubic centimeters (7.2 ounces with a specific gravity of 1.0) capacity.

Effect of temperature of the heating medium. Starting from the base configuration, an analysis is carried out to evaluate the impact of changes in the temperature of the heating medium (T_∞). As the convection oven free-stream temperature is increased, the heating time for the food decreases significantly. However there are several factors that need to be considered, The food mass must not be permitted to have any hot spots showing temperatures in excess of 83° C (180° F) [4]. This introduces a limitation on the temperatures that the gases in the convection oven may attain.

For the large can, as seen in Figure 10, a reduction of convection oven gas temperatures to 77° C (170° F) limits the cold-spot temperature to 59° C (138° F) and the hot-spot temperature to 69° C (156° F). This narrow range of 10° C coupled with a heating period of 0.78 hours is a desirable condition and consequently a convection oven free-stream temperature of 77° C (170° F) is assumed in all subsequent analysis.

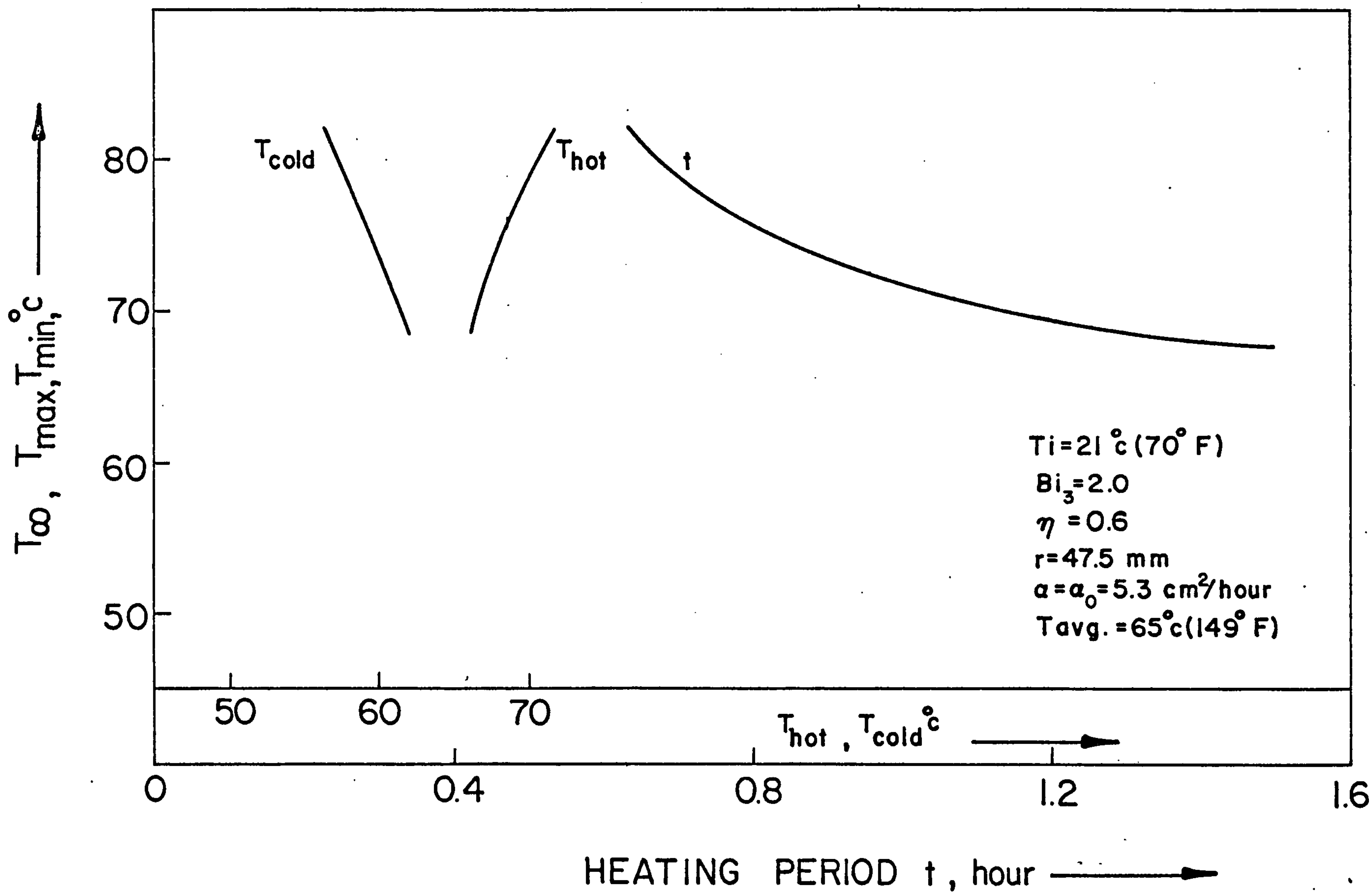

Figure 10 Effect of Temperature of the Heating Medium.

Effect of aspect ratio. The dependence of the heating period and of the cold-spot and the hot-spot temperatures differential on the aspect ratio has been studied for two different can sizes. The first case relates to a large can (a volume of 204 cm^3) and the second case relates to a small can (a volume of 86 cm^3).

Figures 11a and 11b show that the aspect ratios between 0.6 and 1.4 do not have any significant effect on the heating time. The heating time decreases considerably for an aspect ratio on either side of this range. The differential between the hot-spot and cold-spot temperatures increases however with the aspect ratio. An aspect ratio of 0.6 is used in further parametric analysis.

For a large can, this aspect ratio results in the values of cold-spot and hot-spot temperatures as 59°C (138°F) and 69°C (156°F) respectively; a differential of 10°C (18°F). The heating period is 0.78 hours (Figure 11a).

For a small can, an aspect ratio of 0.6 results in the values of cold-spot and hot-spot temperatures as 59°C (138°F) and 70°C (158°F) respectively; a differential of 10°C (18°F). The heating period is 0.45 hours (Figure 11b).

Effect of convection heat transfer coefficient. The increase in convection heat transfer coefficient results in a decreased heating period but an increase in the hot-spot and the cold-spot temperature differential. Figure 12 shows the results obtained for the large can. It should be noted that, for the large can, assuming the values of convection heat transfer

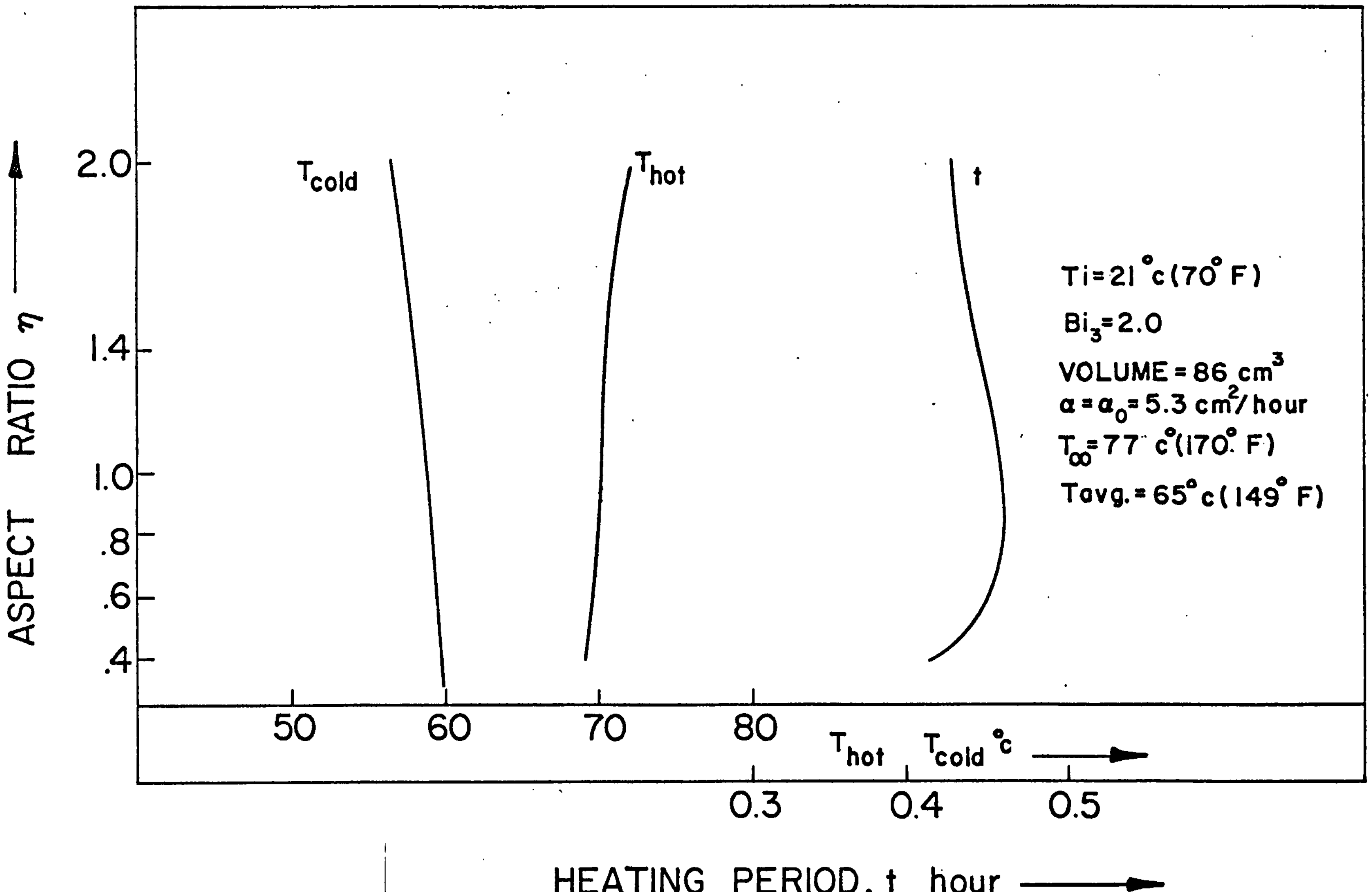

Figure 11a Effect of Aspect Ratio of Food Can: Volume 86 cubic centimeters

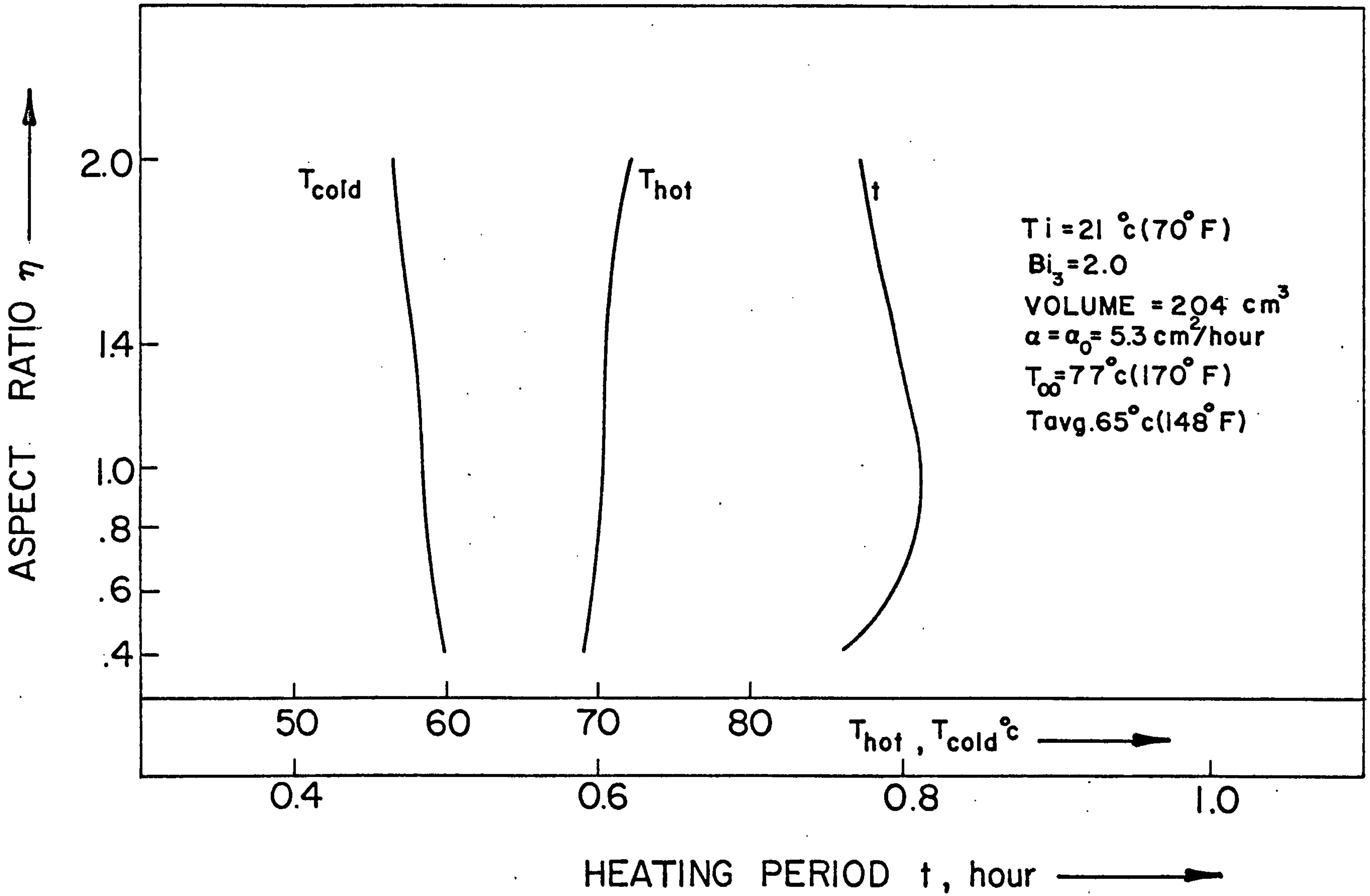

Figure 11b Volume 204 cubic centimeters

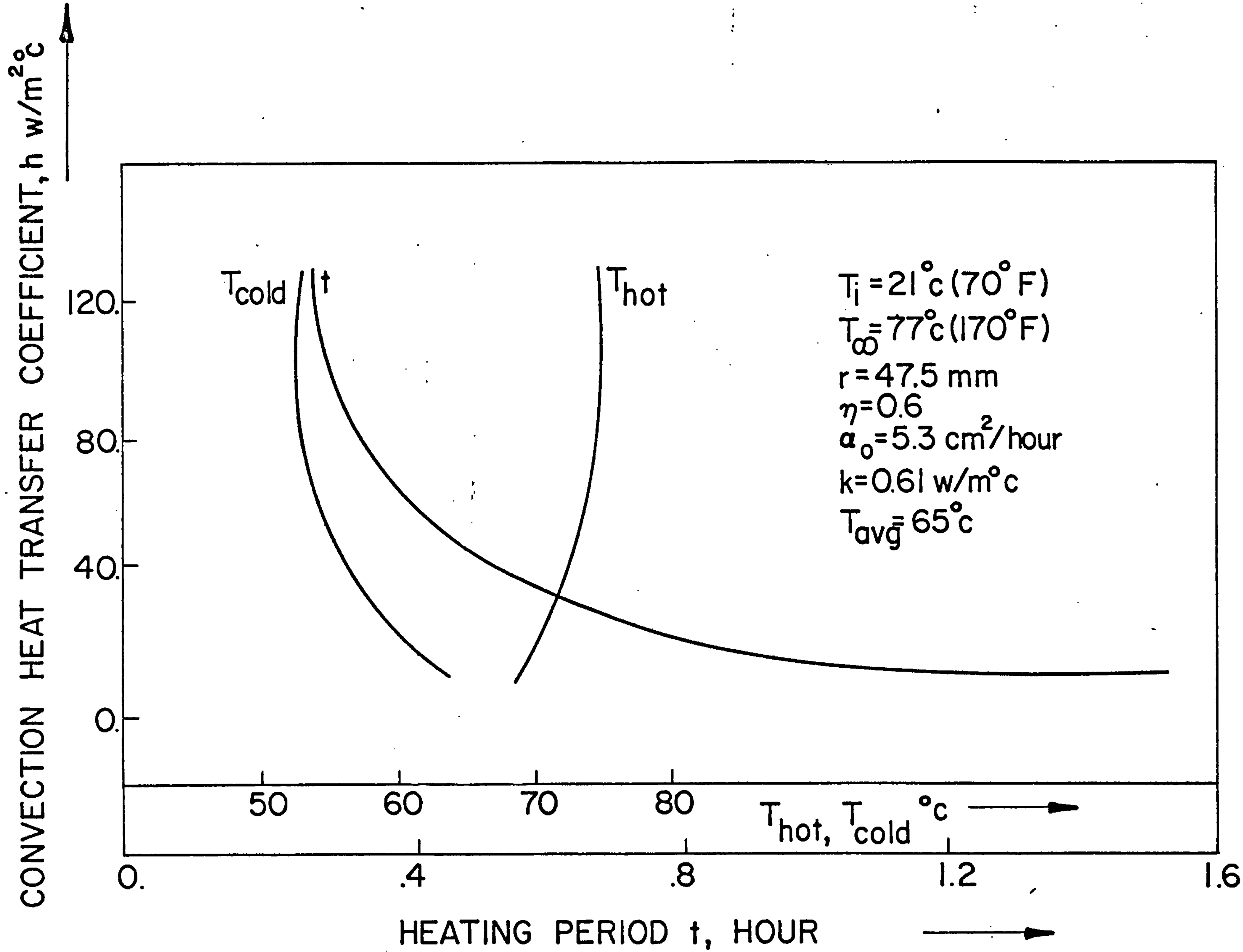

Figure 12 Effect of the Convection Heat Transfer Coefficient of the Heating Medium.

coefficients as 22-33 Watts/m^2°C (4-6 Btu/hr ft^2°F);or a Biot number range of 1.7 to 2.6. A value for Biot number has been assumed as 2.5. The corresponding value of heat transfer coefficient then becomes 32 Watts/m^2°C (5.7 Btu/hr ft^2°F). From Figure 12, the hot-spot and cold-spot temperatures are obtained as 58°C (136°F) and 71°C (160°F) respectively; a differential of 13°C (24°F). The heating period is 0.65 hour.

Effect of thermal diffusivity. As discussed earlier, the reliability of published material on thermophysical data for nutrient materials is questionable. Moreover, the thermal diffusivity for most nutrient materials is close to that of water. Hence a dimensionless ratio α/α_0 is used as an independent variable while plotting these charts; where α_0 is the thermal diffusivity of water at standard conditons. Figure 13 shows that an increase in thermal diffusivity reduces the heating period for food as would be expected. As discussed earlier, chili has an upper limiting value of thermal diffusivity among thermostabilized foods (α for chili is 5.63 cm^2/ hour). The heating period for a large can of chili will be 0.61 hour. Similarly, stewed tomatoes, which has the lower limiting value of thermal diffusivity among thermostabilized foods (α for stewed tomatoes is 5.00 cm^2/ hour), will be heated in a period of 0.69 hour.

Recommended Configuration

The recommendation is based on assumptions stated in guidelines later modified by the results of parametric

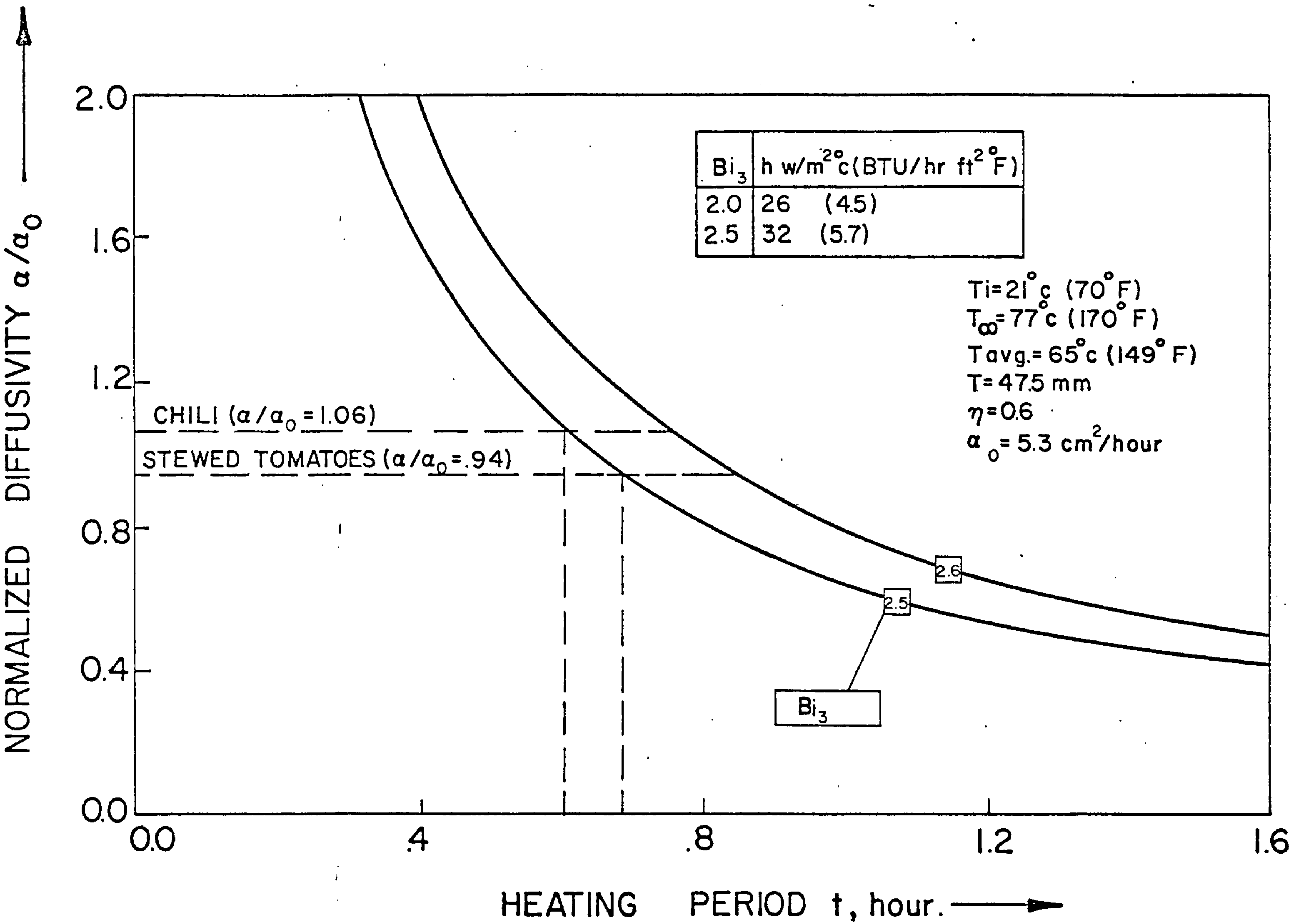

Figure 13 Effect of Thermal Diffusivity of Food

analysis. The values of important parameters like the hot-spot and cold-spot temperatures and the heating period are calculated for the recommended configuration in case of a large can having a volume of 204 cubic centimeters and a small can having a volume of 86 cubic centimeters of food. The summarized results are shown in Table 3.

Table 3. Recommended Configurations

1. ASSUMED VARIABLES:	1) Intitial temperature - 21°C (70°F) 2) Average temperature after heating - 65°C (149°F) 3) Thermal diffusivity of water at standard conditions - 5.3 cm^2/hr 4) Internal conductance - 0.61 Watts/m°C
2. RECOMMENDED PARAMETER VALUES:	1) Convection heat transfer coefficient - 32 Watts/m^2°C (5.7 Btu/hr ft^2°F) 2) Aspect ratio - 0.6 3) Temperature of heating gas- 77°C(170°F)
3. SATISFACTORY RESULTS: (a) LARGE CAN OF FOOD	1) Diameter - 95 millimeter (3-3/4inch) 2) Length - 28.5 millimeter (1-1/8 inch) 3) Period of heating -0.65 hour 4) Time spent in temperature range of bacterial growth - 0.5 hour 5) Hot-spot temperature - 71°C (160°F) 6) Cold-spot temperature - 58°C (136°F)

Table 3 (Continued)

(b) SMALL CAN OF FOOD	1) Diameter - 72 millimeter (2-13/16 inch)
	2) Length - 21.5 millimeter (27/32 inch)
	3) Period of heating - 0.45 hour
	4) Hot-spot temperature - 69.5°C (157°F)
	5) Cold-spot temperature- 59.5°C (139°F)

7. RECOMMENDATIONS FOR FURTHER RESEARCH

Assumptions

The present analysis is based on the assumptions that an axisymmetric internal heat transfer process is involved and that uniform heat transfer coefficients are present at all can surfaces. In the actual heater design, it may be difficult to meet these criteria. The following discussion is related to the impact of these assumptions and further work that may be done in this area to supplement the present findings.

Average heat transfer coefficient. The average heat transfer coefficient on any surface of the food can is given as

$$\bar{h}_i = \frac{1}{A_i} \int h_i dA$$

where

A_i is the area of can surface under consideration,

h_i is the local convection heat transfer coefficient,

$\bar{h}_i$ is the average heat transfer coefficient.

The average values $\bar{h}_1$, $\bar{h}_2$, $\bar{h}_3$ are to be substituted in place of h_1, h_2 and h_3. The heat transfer analysis shall be carried out as usual. Results of an experiment in a convection oven , when available, should be compared to the numeric solutions derived in the present study. The present analysis will also be helpful in optimizing the oven design.

Axisymmetry. Effort should be made in the heater design to obtain close approach to an axisymmetric heating process. All deviations would add to uneven heating and inefficient utilization of available thermal energy.

Food-mix Study

The actual food system for a space shuttle contains thermostabilized food, dehydrated food and frozen food. Since the heating times for the three types of food are different, a study may determine which of the following alternatives is the most desired one:

1. Temperature sensing element for individual food can (or packages) that can activate when a particular can (or package) reaches the desired temperature.

2. A single timer control that can be programmed for the food requiring the maximum heating time. The balance of the food will continue to be heated above its desired optimum.

Phase Change for Frozen Food

Frozen food requires larger heating time since the average temperature in an element of food mass stabilizes when melting starts and is maintained constant until the entire element changes into a liquid stage.

The finite-difference solution can be modified so that the temperature of a node at melting point remains constant until an energy equal to the latent heat of fusion is supplied. The temperature at the node becomes a dependent variable in the system again.

APPENDIX A

SOLUTION OF EQUATIONS OF HEAT CONDUCTION IN CYLINDRICAL COORDINATES

The homogenous linear partial differential equations of heat conduction repeated here for easy reference are

$$\frac{\partial^2\Theta}{\partial r_n^2} + \frac{1}{r_n}\cdot\frac{\partial\Theta}{\partial r_n} + \frac{\partial^2\Theta}{\partial z_n^2} = \frac{\partial\Theta}{\partial Fo} \qquad (2-6)$$

where $\Theta = \Theta(r_n, z_n, Fo)$;

$Fo>0$; $0<r_n<1$; $-0.5\eta<z_n<0.5\eta$.

with initial condition

$$\Theta(r_n, z_n, 0) = 0 \qquad (2-7)$$

and boundary conditions

$$\left.\frac{\partial\Theta}{\partial z_n}\right|_{z_n=0.5\eta} = Bi_1\{\Theta(r_n, -0.5\eta, Fo)-1\} \qquad (2-8)$$

$$\left.\frac{\partial\Theta}{\partial z_n}\right|_{z_n=0.5\eta} = Bi_2\{\Theta(r_n, 0.5\eta, Fo)-1\} \qquad (2-9)$$

$$\left.\frac{\partial\Theta}{\partial r_n}\right|_{r_n=1} = Bi_3\{\Theta(1, z_n, Fo) -1\} \qquad (2-10)$$

Solution by Separation of Variables

Assume a separation of variables in the form

$$\Theta(r_n, z_n, Fo) = R(r_n).Z(z_n).F(Fo) \qquad (A-1)$$

The differential equation (2-6) becomes

$$\frac{1}{R}\left\{\frac{d^2R}{dr_n^2} + \frac{1}{r_n}\frac{dR}{dr_n}\right\} + \left\{\frac{1}{Z}\frac{d^2Z}{dz_n^2}\right\} = \left\{\frac{1}{F}\frac{dF}{dFo}\right\} \qquad (A-2)$$

Since the functions R, Z and F are independent of each other, equation A-2 is satisfied only if each expression inside the square bracket is equal to a constant; that is

$$\frac{1}{F}\frac{dF}{dFo} = -\lambda^2 \qquad \text{(A-3a)}$$

$$\frac{1}{Z}\frac{d^2Z}{dz_n^2} = -\mu^2 \qquad \text{(A-3b)}$$

where λ and μ are the separation parameters and are constants. Then R function satisfies

$$\left(\frac{d^2R}{dr_n^2} + \frac{1}{r_n}\frac{dR}{dr_n}\right) + \beta^2 R = 0 \qquad \text{(A-3c)}$$

where $\beta^2 = \lambda^2 - \mu^2$

Equations (A-3a), (A-3b) and (A-3c) have particular solutions in the form

$$F = \exp\{-(\beta^2+\mu^2)Fo\} \quad Z: \begin{matrix}\sin \mu z_n \\ \cos \mu z_n\end{matrix} \quad R: \begin{matrix}Jo\ (\beta r_n) \\ Yo\ (\beta r_n)\end{matrix} \qquad \text{(A-4)}$$

where Jo, Yo are zero-order Bessel functions of the first and second kind respectively.

It should be noted that β_i and μ_j are roots of equations $\beta J_1\ (\beta) = Jo\ (\beta)\ Bi_1$ and $\cot \mu = \frac{\mu^2 - Bi_2^2}{2\mu Bi_2^2}$ respectively

$$\Theta = \sum_{i=1}^{\infty}\sum_{j=1}^{\infty} A_i B_j Jo(\beta_i r_n)\cdot\cos(\mu_j z_n)\cdot\exp\{-(\beta_i^2+\mu_j^2)Fo\} \qquad \text{(A-5)}$$

A_i and B_j are constant coefficients that can be determined by a simplifying assumption that the Biot numbers for the two face surfaces are identical that is $Bi_1 = Bi_2$. Then applying the technique of product solutions treated by Luikov [6],

$$A_i = \frac{2\ Bi_3}{Jo(\beta_i)(\beta_i^2+Bi_3^2)},$$

$$B_j = (-1)^{j+1}\frac{2\ Bi_1(Bi_1^2+\mu_j^2)^{0.5}}{\mu_j(Bi_1^2+Bi_1+\mu_j^2)}.$$

The average temperature of a finite cylinder is found by the formula

$$\bar{\theta}(Fo) = \frac{1}{\pi(1)^2\eta} \cdot \int_0^{\eta} \int_0^{\eta} \pi r_n \; \theta(r_n, z_n, Fo) dr_n dz_n.$$

If instead of θ, the corresponding solution is substituted, upon integration we obtain

$$\bar{\theta}(Fo) = \sum_{i=1}^{\infty} \sum_{j=1}^{\infty} C_i D_j \exp\{-(\beta_i^2 + \mu_j^2) Fo\} \qquad \text{(A-6)}$$

where

$$C_i = \frac{4Bi_3^2}{\beta_i^2(\beta_i^2 + Bi_3^2)};$$

$$D_j = \frac{2Bi_1^2}{\mu_j^2(Bi_1^2 + Bi_1 + \mu_j^2)}.$$

Solution by Operational Method

Case of an infinite plate. The equations of heat conduction for the present case of one-dimensional heat conduction are

$$\frac{\partial^2\theta}{\partial z_n^2} = \frac{\partial\theta}{\partial Fo} \qquad \text{(A-7)}$$

with $\theta = \theta(z_n, Fo)$; $Fo > 0$; $-0.5\eta < z_n < 0.5\eta$.

with initial condition

$$\theta(z_n, 0) = 0$$

and boundary conditions

$$\left.\frac{\partial\theta}{\partial z_n}\right|_{z_n=-0.5\eta} = Bi_1\{\theta(-0.5\eta, Fo) - 1\}$$

$$\left.\frac{\partial\theta}{\partial z_n}\right|_{z_n=0.5\eta} = -Bi_1\{\theta(0.5\,\eta, Fo) - 1\}$$

A solution of differential equation (A-7) using Laplace transform may be written, reference [6] , as

$$\tilde{\theta}(z_n,s) = A \cos h(s)^{0.5} z_n + B \sin h\,(s)^{0.5}\; z_n. \qquad \text{(A-8)}$$

Boundary conditions for the transform will be of the form

$$-\tilde{\theta}'(\eta/2,s) + \frac{2Bi_1}{\eta}\{(1/s) - \theta(\eta/2,s)\} = 0 \qquad \text{(A-9)}$$

$$\tilde{\theta}'\,(0,s) = 0 \qquad \text{(A-10)}$$

where

$$\tilde{\theta}\,(z_n,s) = L\,\{\theta(z_n,Fo)\}$$

$$= \int_0^\infty \theta(z_n,Fo)e^{-sFo}\,dFo,$$

$$\theta(z_n,\,Fo) = L^{-1}\,\{\tilde{\theta}(z_n,\,s)\}$$

$$= \frac{1}{2\pi i}\int_{\sigma-i\infty}^{\sigma+i\infty} \tilde{\theta}'(z_n,s)e^{sFo}\,ds.$$

and $\tilde{\theta}'$ is differential of $\tilde{\theta}$.

From the symmetry condition (A- 8) it follows that B = 0 (the temperature distribution is symmetrical with respect to the center line).

We substitute solution (A-8) into boundary condition (A-9) to obtain:

$$-A\,S^{0.5}\,\sin h\,S^{0.5}\,\frac{\eta}{2} + \frac{2\,Bi_1}{\eta} - \frac{2\,Bi_1}{\eta}\,A\,\operatorname{Cos} h\,S^{0.5}\,\frac{\eta}{2} = 0$$

thence, the constant A is defined as

$$A = \frac{1}{s(\operatorname{Cos} h\,S^{0.5}\,\frac{\eta}{2} + \frac{\eta}{2Bi_1}\sin h\,S^{0.5}\,\frac{\eta}{2})} \qquad \text{(A-11)}$$

Thus, the solution for the transform will be

$$\tilde{\theta}(z_n,s) = \frac{\operatorname{Cosh} S^{0.5}\cdot z_n}{s(\operatorname{Cos} h\,S^{0.5}\,\frac{\eta}{2} + \frac{2Bi_1}{\eta}\,S^{0.5}\,\sinh S^{0.5}\,\frac{\eta}{2})} = \frac{\Phi(s)}{\Psi(s)} \qquad \text{(A-12)}$$

Using the theorem of expansion, reference [6]

$$\theta(z_n, Fo) = \sum_{j=1}^{\infty} \frac{\Phi(s_j)}{\Psi'(s_j)} e^{s_j Fo} \tag{A-13}$$

where S_j are simple roots of the function $\Psi(s)$.

In our case (1) s=1 (zero root) and (2) an infinite number of roots S_j determined by the equation

$$\operatorname{Cot} \mu = \frac{\mu}{Bi_1} \tag{A-14}$$

where

$$\mu = i\, s^{0.5}_{\frac{n}{2}}$$

Since

$$\Psi'(0) = 1 \text{ and}$$

$$\Psi'(s_j) = -\frac{\sin \mu_j \operatorname{Cos} \mu_j + \mu_j}{2 \sin \mu_j}$$

In addition

$$\Phi(0) = 1$$

$$\Phi(s_j) = \operatorname{Cos} \mu_j z_n$$

Finally, by (A-13)

$$\theta(z_n, Fo) = 1 - \sum_{j=1}^{\infty} B_j \operatorname{Cos} (\mu_j z_n) \exp(-\mu_j^2 Fo) \tag{A-15}$$

where

$$Bj = (-1)^{j+1} \frac{2Bi_1 (Bi_1^2 + \mu_j^2)^{0.5}}{\mu_j (Bi_1^2 + Bi_1 + \mu_j^2)} .$$

<u>Case of an Infinite Cylinder</u>. The differential heat conduction equation for an infinite cylinder is written as

$$\frac{\partial^2 \theta}{\partial r_n^2} + \frac{1}{r_n} \frac{\partial \theta}{\partial r_n} = \frac{\partial \theta}{\partial Fo} \tag{A-16}$$

$$(\theta > 0;\ 0 < r_n < 1)$$

with initial condition

$$-\theta(r_n, 0) = 0 \tag{A-17}$$

and boundary conditions

$$-\frac{\partial\Theta(1,Fo)}{\partial r_n} = Bi_3\{\Theta(1,\ Fo) - 1\}, \qquad (A\text{-}18)$$

$$\frac{\partial\Theta(0,Fo)}{\partial r_n} = 0,\ \Theta(0,\ Fo) \neq \infty \qquad (A\text{-}19)$$

It can be shown, that for a symmetric problem, a solution for the transform $\tilde{\Theta}(r_n,s)$ has the form (A-20)

$$\tilde{\Theta}(r_n,\ s) = AIo\cdot(S^{0.5}r_n)$$

where A is a constant independent of r_n and $Io\{s^{0.5}r_n\} = Jo\{is^{0.5}r_n\}$ is the modified zero-th order Bessel function of the first kind. The transition from the ordinary Bessel functions to the modified functions may be made by the relationship

$$I_v(z) = i^{-v}J_v(iz). \qquad (A\text{-}21)$$

The constant A is found from the boundary condition (A-18) which transform to the form

$$-\tilde{\Theta}'(1,\ s) = Bi_3\{\Theta(1,s) - 1/s\} \qquad (A\text{-}22)$$

By (A-20) and (A-22),

$$A = \frac{1/s}{\left[Io\cdot s^{0.5} + \frac{1}{Bi_3}s^{0.5}\cdot I_1 s^{0.5}\right]},$$

where

$$I_1(z) = Io'(z) = \frac{1}{2}z + \frac{1}{2^2 4}z^3 + \frac{1}{2^2 4^2 6}z^5 + \ldots$$

Hence, solution (A-20) will have the form

$$\tilde{\Theta}(r_n,s) = \frac{S^{0.5}r_n/s}{\left(Io\cdot s^{0.5} + \frac{1}{Bi_3}s^{0.5}\cdot I_1 s^{0.5}\right)} = \frac{\Phi(s)}{\Psi(s)} \qquad (A\text{-}23)$$

Using the theorem of expansion,

$$\tilde{\Theta}(r_n,\ Fo) = \sum_{i=1}^{\infty}\frac{\Phi(si)}{\Psi'(si)}e^{s_i Fo}$$

where s_i are simple roots of the function $\Psi(s)$

since

$$\Psi(s) = s\Phi(s) = 0,$$

and we substitute $s_i = -\beta_i^2$. The constants β_i are determined from the characteristic equation

$$Jo(\beta) - \frac{\beta}{Bi_3} J_1(\beta) = 0. \qquad \text{(A-24)}$$

In addition

$$\frac{\Phi(0)}{\Psi'(0)} = 1,$$

$$\frac{\Phi(s_i)}{\Psi'(s_i)} \exp(s_i\, Fo) = -\frac{2\, Bi_3\, Jo\,(\beta i r_n)}{\{(Bi_3+1)J_1(\beta_i)+\beta_i J_1'(\beta_i)\}\beta_i} \times \exp(-\beta i^2 Fo)$$

since $I_1'(z) = J_1'(i\, z)$

Hence the solution of the problem has the form

$$\Theta = 1 - \sum_{i=1}^{\infty} A_i Jo(\beta_i r_n) \exp(-\beta_i^2 Fo) \qquad \text{(A-25)}$$

where $A_i = \dfrac{2Bi_3}{Jo(\beta_i)\cdot(\beta_i^2+Bi_3^2)}$ (A-26)

<u>Case of a finite Cylinder</u>. It can be shown that the temperature distribution in a cylinder of length η and radius 1 is given by the equation

$$(1-\Theta) = (1-\Theta_1)\,(1-\Theta_2) \qquad \text{(A-27)}$$

where Θ, Θ_1 and Θ_2 are the dimensionless temperatures at a point in the finite cylinder, an infinite plate of thickness η and an infinite cylinder of radius 1 respectively.

The initial and boundary conditions for an infinite cylinder and a plate remain the same as for a cylinder of finite dimensions.

Substituting the values for Θ_1 and Θ_2 calculated earlier in (A-15) and (A-25),

$$\Theta = \sum \sum A_i B_j Jo(\beta_i r_n) Cos(\mu_j z_n) \exp\{-(\beta_i^2+\mu_j^2)Fo\} \qquad \text{(A-28)}$$

which is the same as solution (A-5) obtained earlier.

Solution by the Method of Finite-Integral Transforms

In the absence of internal heat generation and assuming a uniform initial temperature (zero, in dimensionless quantities) in the cylinder, the expression for the special case of axisymmetric heat flow in the analysis by Olcer, expressed in dimensionless variables, in accordance with reference [8] becomes

$$\Theta(r_n, z_n, Fo) = 1-\sum_{i=1}^{\infty}\sum_{j=1}^{\infty} C_i L_j \Phi_i(r_n) X_j(z_n)\cdot$$
$$\exp\{-(\lambda_i^2+\nu_j^2)Fo\} \times \int_0^1\int_{-\eta/2}^{\eta/2} \Phi_i(r_n)X_j(z_n)r_n dr_n dz_n \qquad (A-29)$$

where

$$X_j(z_n) = \cos\nu_j(0.5\eta+z_n)+ \frac{Bi_1}{\nu_j}\sin\nu_j(0.5\eta+z_n) \qquad (A-30)$$

and ν_j is the jth non-negative root of

$$(Bi_1+Bi_2)\nu_j \cos\eta\nu_k=(\nu_j^2-Bi_1 Bi_2)\sin\eta\nu_j$$

The subeigen function $\Phi_i(r_n)$ is defined by

$$\Phi_i(r_n) = \frac{Jo(\lambda_i r_n)}{Jo(\lambda_i)} \qquad (A-31)$$

where Jo(x) is the Bessel function of the first kind of the zero order and argument x, and λ_i is the ith non-negative root of

$$Bi_3 Jo(\lambda_i) = \lambda_i J_1(\lambda_i) \qquad (A-32)$$

and where

$$\frac{1}{C_i} = \frac{\lambda_i^2+Bi_3^2}{2\lambda_i^2}, \qquad (A-33)$$

$$\frac{1}{L_j} = \int_{-\eta/2}^{\eta/2} X_j^2(z_n)\,dz_n$$

$$= 0.5\eta(\nu_j^2+Bi_1^2)(\nu_j^2+Bi_2^2)+0.5(Bi_1+Bi_2)(\nu_j^2+Bi_1Bi_2) \quad (\nu_j\neq 0)$$

$$=\eta \quad (\nu_j=0). \qquad (A-34)$$

APPENDIX B

EXPLICIT FINITE-DIFFERENCE EQUATIONS

Formulation

Finite-difference approximations of temperature derivatives at a node (i,j) by central-difference equations are

$$\left.\frac{\partial\Theta}{\partial r_n}\right|_{i,j} = \frac{\Theta_{i+1,j} - \Theta_{i-1,j}}{2\Delta r_n} + O(\Delta r_n)^2 \qquad \text{(B-1)}$$

$$\left.\frac{\partial\Theta}{\partial z_n}\right|_{i,j} = \frac{\Theta_{i,j+1} - \Theta_{i,j-1}}{2\Delta z_n} + O(\Delta z_n)^2 \qquad \text{(B-2)}$$

$$\left.\frac{\partial^2\Theta}{\partial r_n^2}\right|_{i,j} = \frac{\Theta_{i+1,j} - 2\Theta_{i,j} + \Theta_{i-1,j}}{(\Delta r_n)^2} + O(\Delta r_n)^2 \qquad \text{(B-3)}$$

$$\left.\frac{\partial^2\Theta}{\partial z_n^2}\right|_{i,j} = \frac{\Theta_{i,j+1} - 2\Theta_{i,j} + \Theta_{i,j-1}}{(\Delta z_n)^2} + O(\Delta z_n)^2 \qquad \text{(B-4)}$$

The derivatives of temperature at a point (i,j) at time interval x by finite-forward-difference approximation is

$$\left.\frac{\partial\Theta}{\partial Fo}\right|_{i,j}^{x} \quad \frac{\Theta_{i,j}^{x+1} - \Theta_{i,j}^{x}}{\Delta Fo} + O(\Delta Fo) \qquad \text{(B-5)}$$

Errors in finite-difference approximations. The term involving $O(\Delta r_n)^2$ in equation (B-1) indicates that the truncation error is of the order of second power of the error in radial increment. Similar interpretation is to be made for the remaining equations shown above. It is possible to get better accuracy by selecting smaller incremental values for Δr_n, Δz_n and ΔFo with consequential increase in computation time. A trade-off is suggested between accuracy and computation time and expense.

The magnitude of ΔFo in relation to the magnitudes of Δr_n and Δz_n is important for the stability of the finite-difference model.

Solution of Finite-Difference Equations

An explicit finite-difference formulation for an m x n grid network gives a set of m x n algebraic equations that are solved to determine temperature response during one single time interval. Successive iterations lead to a chronological propagation of temperature response in a grid network from start to end of the heating process.

The following substitutions have been made to simplify the finite-difference equations.

$V_0 = 2/n \, Bi_3 \, Mr(1+\frac{1}{2n})$

$V_1 = (2/m)\eta Bi_1 \, Mz, V_2 = (2/m)\eta \, Bi_2 Mz$,

$V_3 = 1 - 2Mr - 2Mz$

$V_4 = V_3 - V_1, V_5 = V_3 - V_2$,

$V_6 = V_3 - V_0, \; V_7 = V_4 - V_0, \; V_8 = V_5 - V_0.$

where

n = number of divisions along the radius

m = number of divisions along the axis

η = aspect ratio = L/R

Equation of Heat Conduction. The finite-difference approximations are substituted in (2-6) to result in the algebraic equation

$$\frac{\Theta^x_{i+1,j} - \Theta^x_{i,j} + \Theta^x_{i-1,j}}{(\Delta r_n)^2} + \frac{1}{r_n} \frac{\Theta^x_{i+1,j} - \Theta^x_{i-1,j}}{\Delta r_n}$$

$$+ \frac{\Theta^x_{i,j+1} - \Theta^x_{i,j} + \Theta^x_{i,j-1}}{(\Delta z_n)^2} = \frac{\Theta^{x+1}_{i,j} - \Theta^x_{i,j}}{\Delta Fo} \qquad \text{(B-6)}$$

Simplifying (B-6) and by the substitutions $r_n=(i-1)\Delta r_n$,

$$\Theta^x_{i,j} = \Theta^x_{i+1,j}\frac{\Delta Fo}{(\Delta r_n)^2}\{1+\frac{1}{2(i-1)}\}+\Theta^x_{i,j}\{1-\frac{2\Delta Fo}{(\Delta z_n)^2}-\frac{2\Delta Fo}{(\Delta r_n)^2}\}$$

$$+\Theta^x_{i-1,j}\frac{\Delta Fo}{(\Delta r_n)^2}\{1-\frac{1}{2(i-1)}\}+\Theta^x_{i,j+1}\frac{\Delta Fo}{(\Delta z_n)^2}+\Theta^x_{i,j-1}\frac{\Delta Fo}{(\Delta z_n)^2}$$

By the substitutions

$$Mr = \frac{\Delta Fo}{(\Delta r_n)^2},\quad Mz = \frac{\Delta Fo}{(\Delta z_n)^2},\quad V_3 = 1-2M_r-2M_z, \tag{B-7}$$

$$V(i) = Mr\{1+\frac{1}{2(i-1)}\},\quad W(i) = Mr\{1-\frac{1}{2(i-1)}\}, \tag{B-8}$$

the equations reduce to

$$\Theta^{x+1}_{i,j} = \Theta^x_{i+1,j}V(i)+\Theta^x_{i,j}V_3+\Theta^x_{i-1,j}W(i)+\Theta^x_{i,j+1}Mz+$$
$$\Theta^x_{i,j-1}Mz \tag{B-9}$$

The equation derived here can be modified to represent the heat flow along the axis of the cylinder. From the grid network shown in Figure 2, along the axis of the can,

$$i = 1,$$

Also by condition of axisymmetry

$$\Theta_{i+1,j} = \Theta_{i-1,j}.$$

Applying L'Hopital's Rule

$$\frac{1}{r_n}\frac{\partial\Theta}{\partial r_n}\rightarrow\frac{\partial^2\Theta}{\partial r_n^2},\ \text{in the limit as } r_n\rightarrow 0$$

Hence the equation of heat flow along the axis is

$$2\frac{\partial^2\Theta}{\partial r_n^2}+\frac{\partial^2\Theta}{\partial z_n^2} = \frac{\partial\Theta}{\partial Fo}. \tag{B-10}$$

or,
$$\Theta^{x+1}_{1,j} = \Theta^x_{2,j}.2Mr+\Theta^x_{1,j+1}.V_3+\Theta^x_{1,j-1}.Mz+\Theta^x_{1,j}.V_3$$
$$+(\Theta^x_{2,j}-\Theta^x_{1,j}).2Mr \tag{B-11}$$

Boundary conditions. Equations (2-8), (2-9) and (2-10) representing the boundary conditions reduce to the following by the finite-difference approximations:

For the bottom face

$$\frac{\theta^x_{i,j+1} - \theta^x_{i,j-1}}{2\Delta z_n} = Bi_1 \cdot (\theta^x_{i,j} - 1), \text{ at } j=1 \qquad \text{(B-12)}$$

For the top surface,

$$\frac{\theta^x_{i,j+1} - \theta^x_{i,j-1}}{2\ \Delta z_n} = -Bi_2 \cdot (\theta^x_{i,j-1}), \text{ at } j=m+1; \qquad \text{(B-13)}$$

and for the lateral cylindrical surface

$$\frac{\theta^x_{i+1,j} - \theta^x_{i-1,j}}{2\Delta r_n} = -Bi_3 \cdot (\theta_{i,j-1}), \text{ at } i=n+1. \qquad \text{(B-14)}$$

since

$$\Delta r_n = 1/n, \ \Delta z_n = \eta/m$$

Simplification and rearrangement of terms in the above equations leads to

$$\theta^x_{i,0} = \theta^x_{i,2} - 2\eta/m \ \ Bi_1(\theta^x_{i,1} - 1) \qquad \text{(B-15)}$$

$$\theta^x_{i,m+2} = \theta^x_{i,m} - 2\ \eta/m \ \ Bi_2(\theta^x_{i,m+1} - 1) \qquad \text{(B-16)}$$

$$\theta^x_{n+2,j} = \theta^x_{n,j} - 2/n \quad Bi_3(\theta^x_{n+1,j} - 1) \qquad \text{(B-17)}$$

Since $Mr = \Delta Fo/(\Delta r_n)^2$, $Mz = \Delta Fo/(\Delta z_n)^2$,

$$V(i) = Mr\{1 + \frac{1}{2(i-1)}\}, \ W(i) = Mr\{1 - \frac{1}{2(i-1)}\} .$$

where the dimensionless parameters are

$$\Delta r_n = \Delta r/R = 1/n, \ \Delta z_n = \Delta z/R = \eta/m, \ \Delta Fo = \alpha\Delta t/R^2$$

Interior node and axial node. The representative equations have been presented earlier in (B-9) and (B-11).

Node at the bottom face. Solving the finite-difference equation for the bottom face (B-15),

$$\Theta^{x}_{i,0} = \Theta^{x}_{i,2} - 2\ \eta/m\ Bi_1\ (\Theta^{x}_{i,1} - 1) \qquad \text{(B-18)}$$

Substituting the value for $\Theta_{i,0}$ in (B-9)

$$\Theta^{x+1}_{i,0} = \Theta^{x}_{i+1,1}.Mr\{1+\frac{1}{2(i-1)}\} + \Theta^{x}_{i,1}\{1-2Mr-2Mz-2\frac{\eta}{m}Bi_1 Mz\}$$

$$+\Theta^{x}_{i-1,1}\ Mr\{1-\frac{1}{2(i-1)}\} + \Theta^{x}_{i,2}.2Mz + 2\frac{\eta}{m}\ Bi_1\ Mz$$

$$=\Theta^{x}_{i+1,1}.V(i)+\Theta^{x}_{i,1}.V_4 + \Theta^{x}_{i-1,1}.W(i)+\Theta^{x}_{i,2}2Mz+V_1 \qquad \text{(B-19)}$$

Node at the top face. Solving the finite-difference equation for the top face (B-16)

$$\Theta^{x}_{i,m+2} = \Theta^{x}_{i,m} - 2\frac{\eta}{m}\ Bi_2\{\Theta^{x}_{i,m+1} - 1\} \qquad \text{(B-20)}$$

Substituting the values of $\Theta_{i,m+2}$ in equation (B-16)

$$\Theta^{x+1}_{i,m+1} = \Theta^{x}_{i+1,m+1}\ Mr\{1+\frac{1}{2(i-1)}\}+\Theta^{x}_{i,m+1}(1-2Mr-2Mz-2\frac{\eta}{m}Bi_2 Mz)$$

$$+\Theta^{x}_{i-1,m+1}\ Mr\{1-\frac{1}{2(i-1)}\} +\Theta^{x}_{i,m}\ 2Mz+2\frac{\eta}{m}\ Bi_2\ Mz$$

$$=\Theta^{x}_{i+1,m+1}V(i)+\Theta^{x}_{i,m+1}V_5 +\Theta^{x}_{i-1,m+1}W(i)+\Theta^{x}_{i,m}\ 2Mz+V_2 \qquad \text{(B-21)}$$

Node at the lateral cylindrical surface. Solving the finite-difference equation for the lateral surface (B-17)

$$\Theta^{x}_{n+2,j} = \Theta^{x}_{n,j} - 2/n\ Bi_3\{\Theta^{x}_{n+1,j} - 1\} \qquad \text{(B-22)}$$

Substituting the value of $\Theta_{n+2,j}$ in equation (B-9)

$$\theta^{x}_{n+1,j} = \theta^{x}_{n+1,j}\{1-2Mr-2Mz-2/n\ Bi_3\ Mr\ (1+ \frac{1}{2(i-1)})\}$$

$$+\theta^{x}_{n,j}\ 2Mr+ \theta^{x}_{n+1,j+1}\ Mz+ \theta^{x}_{n+1,j-1}\ Mz$$

$$+ 2/n\ Bi_3\ \ Mr\{1+ \frac{1}{2(i-1)}\}$$

$$=\theta^{x}_{n+1,j}V_6+\theta^{x}_{n,j}2Mr+\theta^{x}_{n+1,j+1}Mz+\theta^{x}_{n+1,j-1}Mz+V_0 \quad \text{(B-23)}$$

Node at the bottom corner. Solving equation (B-18) of the bottom face at the specific node (i=n+1,j=1)

$$\theta^{x+1}_{n+1,1} = \theta^{x}_{n+2,1}V(i)+\theta^{x}_{n+1,1}V_4+\theta^{x}_{n,1}W(i)+\theta^{x}_{n+1,2}2Mz+V_1 \quad \text{(B-24)}$$

From equation (B-23) of the lateral surface, at the specific node

$$\theta^{x}_{n+1,1} = \theta^{x}_{n+1,1}V_6+\theta^{x}_{n,1}2Mr+\theta^{x}_{n+1,2}Mz+\theta^{x}_{n+1,0}Mz+V_0 \quad \text{(B-25)}$$

From equation (B-9) of the interior node

$$\theta^{x}_{n+1,1} = \theta^{x}_{n+2,1}V(i)+ \theta^{x}_{n+1,1}V_3+\theta^{x}_{n,1}W(i)+\theta^{x}_{n+1,2}Mz+\theta^{x}_{n+1,0}Mz \quad \text{(B-26)}$$

The terms in equation (B-26) related to the points exterior to the region, $\theta_{n+2,1}$ and $\theta_{n+1,0}$, are eliminated by substitution from (B-24) and (B-25) respectively

$$\theta^{x}_{n+1,1} = \theta^{x}_{n+1,1}V_7+\theta^{x}_{n,1}2Mr+\theta^{x}_{n+1,2}2Mz+V_1+V_0 \quad \text{(B-27)}$$

Node at the top corner. Solving equation for the top face (B-21),

$$\theta^{x+1}_{n+1,m+1} = \theta^{x}_{n+2,m+1}V(i)+\theta^{x}_{n+1,m+1}V_5+\theta^{x}_{n,m+1}W(i)$$

$$+ \theta^{x}_{n+1,m}2Mz+V_2 \quad \text{(B-28)}$$

Solution of equation (B-23) for the lateral surface gives

$$\Theta^{x+1}_{n+1,m+1} = \Theta^{x}_{n+2,m+1}V_6+\Theta^{x}_{n,m+1}2Mr+\Theta^{x}_{n+1,m+2}Mz+\Theta^{x}_{n+1,m}Mz+V_0 \tag{B-29}$$

Solution of equation (B-9) for an interior node gives

$$\Theta^{x+1}_{n+1,m+1} = \Theta^{x}_{n+2,m+1}V(i)+\Theta^{x}_{n+1,m+1}V_3+\Theta^{x}_{n,m+1}W(i)$$

$$+\ \Theta^{x}_{n+1,m+2}Mz+\Theta^{x}_{n+1,m}Mz \tag{B-30}$$

The terms in equation (B-30) related to points exterior to the region, $\Theta_{n+2,m+1}$ and $\Theta_{n+1,m+2}$, are eliminated by substitution from (B-28) and (B-29) respectively

$$\Theta^{x+1}_{n+1,m+1} = \Theta^{x}_{n+1,m+1}V_8+\Theta^{x}_{n+1,m}2Mz+\Theta^{x}_{n,m+1}2Mr+V_2+V_0 \tag{B-31}$$

Node at the intersection of the axis with the bottom face.

The nodal point has grid coordinates

$i=1,\ j=1$

By the assumption of axisymmetry

$$\Theta_{0,1} = \Theta_{2,1}$$

Simplifying equation for the bottom face (B-19)

$$\Theta^{x+1}_{1,1} = \Theta^{x}_{2,1}2Mr+\Theta^{x}_{1,1}V_4+\Theta^{x}_{1,2}2Mz+V_1 \tag{B-32}$$

Node at the intersection of the axis with the top face. The solution is obtained by simplifying the equation for the top face

$$\Theta^{x+1}_{1,m+1} = \Theta^{x}_{2,m+1}2Mr+\Theta^{x}_{1,m+1}V_5+\Theta^{x}_{1,m}2Mz+V_2 \tag{B-33}$$

Stability Criteria

The finite-difference equation may be rewritten as follows:

$$\Theta_{i,j}^{x+1} = a.\Theta_{i,j}^{x} + \Phi(\Theta_{i\pm1,j}^{x} + \Theta_{i,j\pm1}^{x}) \quad (B-34)$$

The solution will be stable if and only if 'a' is a positive number. It will be sufficient to show that a negative value of 'a' will cause an unstable solution.

Let, if possible, 'a' have a negative value. Then a larger value of the present temperature $\Theta_{i,j}^{x}$ will cause a smaller value of the future temperature $\Theta_{i,j}^{x+1}$ This will be in violation of the thermodynamic principle. The computed values of the temperatures will oscillate with an increasing magnitude as the computation progresses in case of instability, Reference [10].

Thus, we can establish a set of criteria to be satisfied so that the complete set of finite-difference equations is stable. Table B-1 shows that some of the stability criteria are redundant.

TABLE B-1 Stability Criteria

Finite-difference equation no.	Stability
(B-11)	$V_3 \geq 0 \quad 1-2\frac{\Delta Fo}{(\Delta r_n)^2} - 2\frac{\Delta Fo}{(\Delta z_n)^2} \geq 0$: Redundant
	$V_3 \geq 0$:Redundant
(B-19)	$V_4 \geq 0 \quad 1-\frac{2\Delta Fo}{(\Delta r_n)^2} - \frac{2\Delta Fo}{(\Delta z_n)^2} - 2/m\ \eta\ Bi_1 . \frac{\Delta FO}{(\Delta z_n)^2} \geq 0$: Redudant
(B-21)	$V_5 \geq 0 \quad 1-\frac{2\Delta Fo}{(\Delta r_n)^2} - \frac{2\Delta Fo}{(\Delta z_n)^2} - 2/m\ \eta\ Bi_1 \cdot \frac{\Delta Fo}{(\Delta z_n)^2} \geq 0$: Redudant
(B-23)	$V_6 \geq 0 \quad 1-\frac{2\Delta Fo}{(\Delta r_n)^2} - 2\frac{\Delta Fo}{(\Delta z_n)^2} - 2/n \cdot Bi_3 \frac{\Delta Fo}{(\Delta r_n)^2} \cdot (1+\frac{1}{2n}) \geq 0$ (B-35)

TABLE B-1 Stability Criteria(Continued)

Finite-difference equation no.		Stability
(B-27)	$V_7 \geq 0$	$1 - 2\frac{\Delta Fo}{(\Delta r_n)^2} - 2\frac{\Delta Fo}{(\Delta z_n)^2} - 2/m\ \eta\ Bi_1 \frac{\Delta Fo}{(\Delta z_n)^2} - 2/n \cdot Bi_3 \frac{\Delta Fo}{(\Delta r_n)^2}(1+\frac{1}{2n}) \geq 0$ (B-36)
(B-31)	$V_8 \geq 0$	$1 - 2\frac{\Delta Fo}{(\Delta r_n)^2} - \frac{2\Delta Fo}{(\Delta z_n)^2} - 2/m\ \eta\ Bi_2 \frac{\Delta Fo}{(\Delta z_n)^2} - 2/n \cdot Bi_3 \frac{\Delta Fo}{(\Delta r_n)^2}(1+\frac{1}{2n}) \geq 0$ (B-37)
(B-32)	$V_4 \geq 0$	: Redundant
(B-33)	$V_5 \geq 0$	: Redundant

Table B-1 shows that the criteria (B-35, B-36 and B-37), if satisfied, will ensure stability. This is achieved by making the finite time element ΔFo sufficiently small. In the computer program, a stability check is done before the computation can progress.

APPENDIX C
COMPUTER PROGRAM

The explicit finite difference equations shown in Appendix B are used to design a computer program.

Introduction to the Program

A program in FORTRAN V was written and run on UNIVAC 1100 Executive 8 system at the University of Houston Computing Center. The variables used in the program HTFLOW are identified in Table C-1.

Table C-1. VARIABLES IN THE HTFLOW PROGRAM

Variable	Definition	Symbol in Text
AMR	Variable in finite-difference scheme	Mr
AMZ	Variable in finite-difference scheme	Mz
B	Range of values for Biot number	
BI1	Biot number, bottom face	Bi_1
BI2	Biot number, top face	Bi_2
BI3	Biot number, lateral cylindrical surface	Bi_3
B1	Variable same as BI1	
B2	Variable same as BI2	
B3	Variable same as BI3	
DELFO	Incremental dimensionless time	$\Delta F0$
DV	Variable in finite-difference scheme	ΔV
DVSVM	Variable in finite-difference scheme	
E	Range of values for ETA	
ETA	Ratio length to radius for the cylinder	η
F	Range of values for F0	

TABLE C-1 VARIABLES IN THE HTFLOW PROGRAM (Continued)

FI	Initial time when boundary condition is transient	
FII	Final Time when boundary condition becomes transient	
FIII	Final time when heat flow across the boundaries is zero	
FO	Time, Dimensionless ($Fo=\alpha t/R^2$)	Fo
FOMAX	Maximum time of run, dimensionless	$\Delta Fomax$
FPTR	Variable in finite-difference scheme	
I	Variable in finite-difference scheme	i
IBSW	Variable that checks for stability criteria	
ICASE	Case number	
ICTR	Iteration count	
IPSW	Variable for stability criteria	
J	Variable in finite-difference scheme	j
K	Variable to select Fo	
KE	Variable to select value of ETA	
LB	Variable to select value of BI1	
M	Number of divisions along the axis	m
MB	Variable to select value of BI2	
MP	M plus one	m+1
N	Number of divisions along the radius	n
NB	Variable to select value of BI3	
NE	Number of ETA Values	
NF	Number of Fo values	
NP	N plus one	n+1
TH	Present temperature, dimensionless	$\Theta_{i,j}^{x}$
THBAR	Average temperature, dimensionless	$\bar{\Theta}$
THMAX	Maximum temperature, dimensionless	Θ_{max}

TABLE C-1 VARIABLES IN THE HTFLOW PROGRAM(Continued)

THSUM	Variable in main program	
TTH	Future temperature, dimensionless	$\Theta_{i,j}^{x+1}$
V	Variable in finite-difference scheme	V(i)
V0 toV8	Variables in finite-difference scheme	V_0 to V_8
W	Variables in finite-difference scheme	W(i)

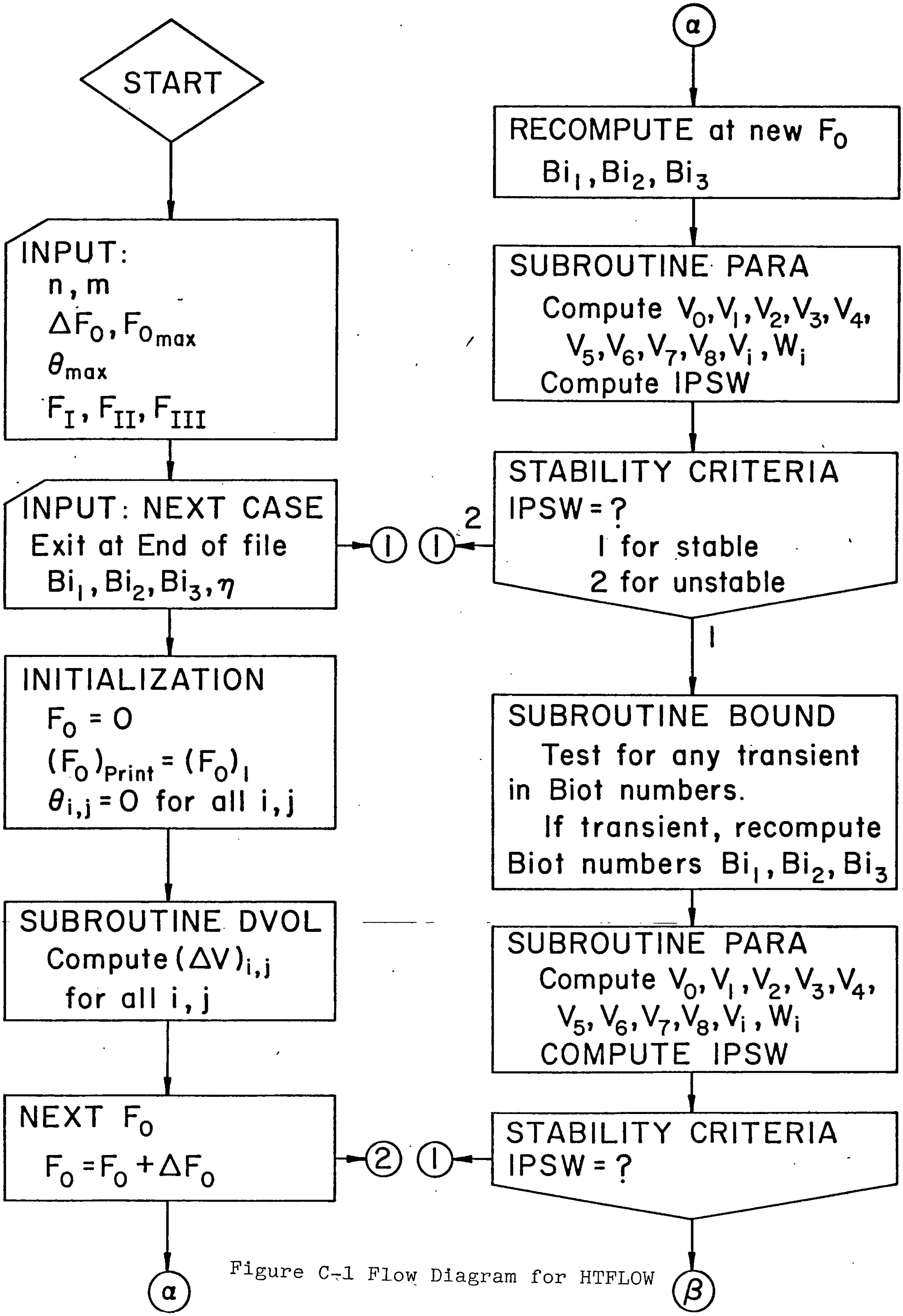

Figure C-1 Flow Diagram for HTFLOW

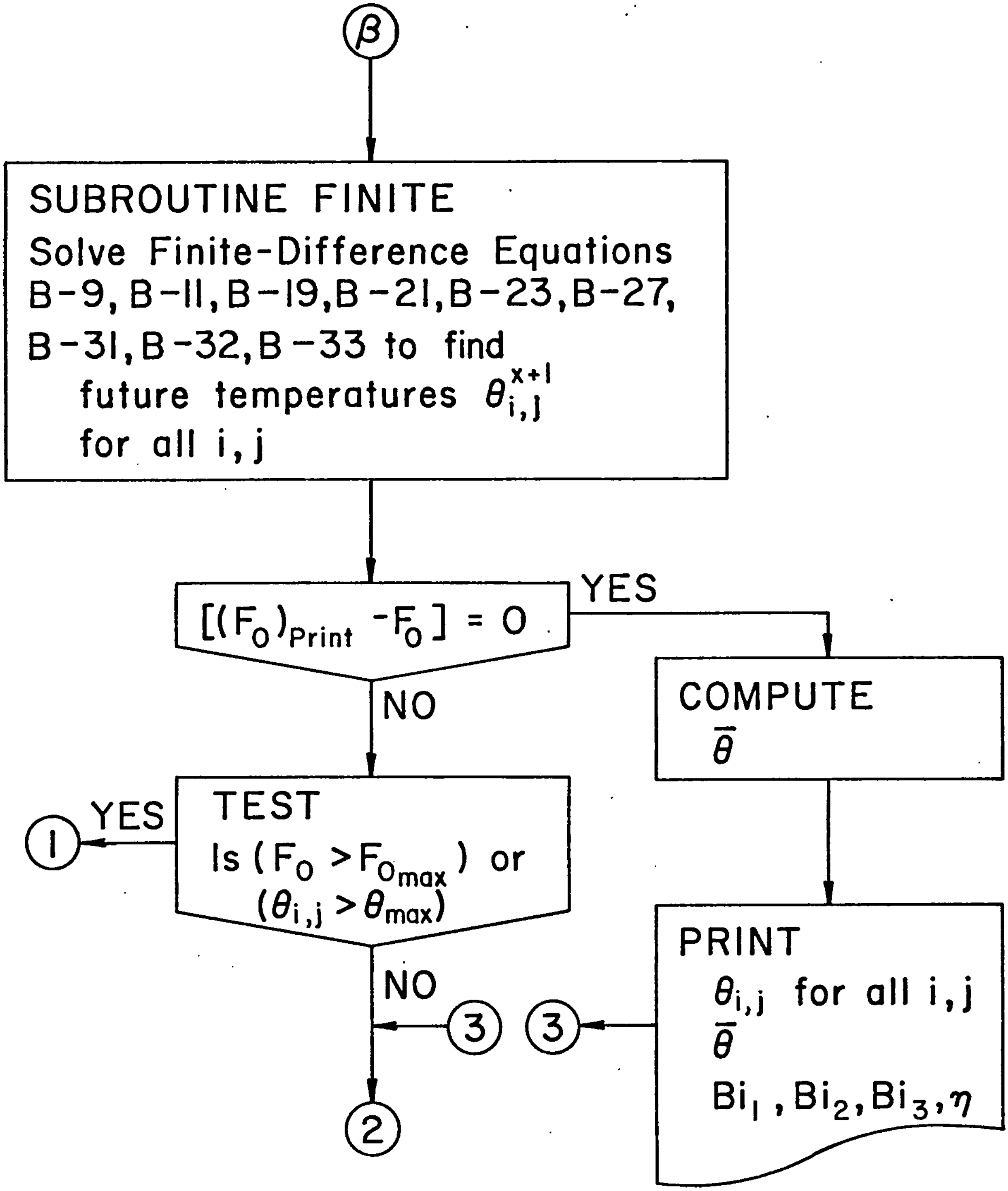

Figure C-1 (Concluded)

Table C-2 Basic content of the main program and Subroutines

Program	
MAIN	See the flow chart
Subroutines	
DVOL	Computes volumes of elements of the grid network in cylindrical coordinate scheme
PARA	Computes a number of parameters for use in equations of finite-difference scheme. Checks for stability criteria
BOUND	Checks for transient stage when Biot numbers may not be steady, as during the start and stop of heat transfer process.
FINITE	Solves by iteration the set of explicit finite-difference equations

Summary listing of Numeric Solutions

Table C-3. Numeric Solutions for Limiting Cases

Case no.[1]	Length of can, mm	Radius of can, mm	Biot Numbers Bi_1	Bi_2	Bi_3	Limiting Case
1	31.75	29.35	.94	.94	.94	
2	317.5	29.35	0	0	.94	Infinite Cylinder[2]
3	58.7	29.35	.094	.094	.094	Short Cylinder[2]
4	31.75	29.35	.01	.01	.01	Low Biot #
5	31.75	29.35	.025	.025	.025	Low Biot #

Note 1. Case numbers assigned to the digital computer outputs

2. Large internal conductance, α=0.0145 cm^2/sec=52 cm^2/hour

Table C-4 Numeric Solutions for Generalized Cases
Small Biot Number ($Bi_3<0.1$), $Bi_1=Bi_2=0.5\ Bi_3\cdot\eta$

Case Numbers [1]	Bi_3	η
35,36,37,38,39,40	.001,.002,.004,.01,.02,.04	0.4
52,53,54,55,56,57	"	0.6
69,70,71,72,73,74	"	0.8
86,87,88,89,90,91	"	1.0
103,104,105,106,107,108	"	1.08
120,121,122,123,124,125	"	1.10
137,138,139,140,141,142	"	1.20
154,155,156,157,158,159	"	1.40
171,172,173,174,175,176	"	1.60
188,189,190,191,192,193	"	2.0
205,206,207,208,209,210	"	4.0
222,223,224,225,226,227	"	6.0
239,240,241,242,243,244	"	10.0

Table C-5, Numeric solutions for Generalized Cases

$Bi_3\geq 0.1$, $Bi_1=Bi_2=0.5\ Bi_3\cdot\eta$

Case Numbers [1]	Bi_3	η
41 to 50	.1,.2,.4,.6,.8,1.0,2.0,4.0,10.0,20.0	0.4
58 to 67	"	0.6
75 to 84	"	0.8
92 to 101	"	1.0
109 to 118	"	1.08
126 to 135	"	1.10
143 to 152	"	1.20

Table C-5, Numeric solutions for Generalized Cases
Continued

160 to 169	.1,.2,.3,.6,.8,1.0,2.0,4.0,10.0,20.0	1.40
177 to 186	"	1.60
194 to 203	"	2.0
211 to 220	"	4.0
228 to 237	"	6.0
245 to 254	"	10.0

Note 1. Case number assigned to digital computer outputs

```
      DIMENSION TH(10,10),V(10),W(10) ,B(50),F(50),DV(10,10),E(50)
  901 FORMAT ('1',30X,'CASE NO.',I4)
 9000 FORMAT (8F10.2)
 9001 FORMAT (8(I5,5X))
 9007 FORMAT (' MODEL UNSTABLE')
 9020 FORMAT (10X,'N=',I5,'  M=',I5)
 9070 FORMAT ( 10X,'DELFO=',F8.3,'  FOMAX=',F8.3,'  FI=',F8.3,'  FII=',
     1                F8.3,'  FIII=',F8.3,'  THMAX=',F8.3)
 9075 FORMAT(' BI VALUES')
 9076 FORMAT(' FO VALUES')
 9077 FORMAT(' ETA VALUES')
 9080 FORMAT (18F7.3)
 9105 FORMAT (10X,' ICTR       FO      BI1      BI2      BI3   THBAR',
     1    5X,'ETA')
 9110 FORMAT (5X,I10,10F8.3)
 9115 FORMAT (18X,10(I5,3X))
 9200 FORMAT (10X,I5,10F8.3)
      READ (5,9001) NE,NB,NF
      READ (5,9000) (B(I),I=1,NB)
      READ (5,9000) (F(I),I=1,NF)
      WRITE (6,9075)
      WRITE (6,9080) (B(I),I=1,NB)
      WRITE (6,9076)
      WRITE (6,9080) (F(I),I=1,NF)
      READ (5,9000) (E(I),I=1,NE)
      WRITE (6,9077)
      WRITE(6,9080) (E(I),I=1,NE)
         ICASE=34
      READ (5,9000) DELFO,FOMAX
      READ (5,9000) FI,FII,FIII
      READ (5,9000) THMAX
      READ (5,9001)N,M
      WRITE (6,9020) N,M
      WRITE (6,9070)      DELFO,FOMAX,FI,FII,FIII,THMAX
         NP=N+1
    3    MP=M+1
    1 READ (5,9001,ERR=3    ,END=5105) LB,MB,NB,KE
         ICASE=ICASE+1
      WRITE (6,901)ICASE
         ETA=E(KE)
C INITIALIZE
   91 FO = 0.
         K=1
         FPRT =F(K)
      DO 101 I=1,NP
      DO 101 J=1,MP
  101 TH(I,J) =0.
      CALL  DVOL(N,M,DV)
   92 FO = FO+DELFO
```

Figure C-2 Listing of Program HTFLOW

```
          BI1=B(LB)*ETA/2.
          BI2=B(MB)*ETA/2.
          BI3=B(NB)
      CALL        PARA (N,M,BI1,BI2,BI3,DELFO,ETA,AMR,AMZ,VO,
     1    V1,V2,V3,V4,V5,V6,V7,V8,V,W,IPSW)
C STABILITY TEST
      IF (IPSW.EQ.1)  GO TO 93
      WRITE(6,9007)
      GO TO 1
   93 CONTINUE
      CALL        ROUND(B1,B2,B3,FO,FI,FII,FIII,
     1     ETA ,BI1,BI2,BI3,IBSW)
      IF (IBSW.EQ.2) GO TO 94
          BI1=B1
          BI2=B2
          BI3=B3
      CALL        PARA (N,M,BI1,BI2,BI3,DELFO,ETA,AMR,AMZ,VO,
     1    V1,V2,V3,V4,V5,V6,V7,V8,V,W,IPSW)
C STABILITY TEST
      IF (IPSW.FQ.1)  GO TO 94
      WRITE(6,9007)
      GO TO 1
   94 CONTINUE
      CALL FINITE (N,M,AMR,AMZ,ETA,TH,VO,V1,
     1 V2,V3,V4,V5,V6,V7,V8,V,W)
      IF ((FPRT-FO).LE..0009) GO TO 95
      GO TO 104
   95 K=K+1
          FPRT =F(K)
          THSUM=0.
          DVSUM=0.
      DO 40 I=1,NP
      DO 40 J=1,MP
          DVSUM=DVSUM+DV(I,J)
         THSUM=THSUM+TH(I,J)*DV(I,J)
   40 CONTINUE
         THBAR=THSUM/DVSUM
      WRITE (6,9105)
      WRITE (6,9110) ICTR,FO,BI1,BI2,BI3,THBAR,ETA
      WRITE (6,9115) (I,I=1,NP)
      DO 103 J=1,MP
  103 WRITE (6,9200) J,(TH(I,J),I=1,NP)
  104 ICTR = ICTR+1
      IF (FO.GT.FOMAX) GO TO 1
      IF (TH(1,4).GT.THMAX) GO TO 1
      GO TO 92
 5105 STOP
      END
```

Figure C-2 (Continued)

```
      SUBROUTINE DVOL(N,M,DV)
      DIMENSION DV(10,10)
         NP=N+1
         MP=M+1
      DO 10 J=2,M
         DV(1,J)=.25
         DV(NP,J)=.5*N
   10 CONTINUE
      DO 20 I=2,N
      DO 20 J=2,M
         DV(I,J)=I-1.
   20 CONTINUE
      DO 30 I=2,N
         DV (I,1)=.5*DV(I,2)
         DV(I,MP)=DV(I,1)
   30 CONTINUE
         DV(NP,1)=.5*DV(NP,1)
         DV(NP,MP)=DV(NP,1)
         DV(1,1)=.5*DV(1,2)
         DV(1,MP)=DV(1,1)
      RETURN
      END
```

Figure C-2(Continued)

```
      SUBROUTINE PARA (N,M,BI1,BI2,BI3,DELFO,ETA,AMR,AMZ,V0,
     1   V1,V2,V3,V4,V5,V6,V7,V8,V,W,IPSW)
      DIMENSION V(10),W(10)
         AMR=N*N*DELFO
         AMZ=DELFO*(M/ETA)**2
         V0=2.*BI3*AMR*(1.+1./(2.*N))/N
         V1=4.*BI1*AMZ/M
         V2=4.*BI2*AMZ/M
         V3=1.-2.*AMR-2.*AMZ
         V4=V3-V1
         V5=V3-V2
         V6=V3-V0
         V7=V4-V0
         V8=V5-V0
      DO 10 I=2,N
         V(I)=AMR*(1.+1./(2.*(I-1)))
         W(I)=AMR*(1.-1./(2.*(I-1)))
   10 CONTINUE
         IPSW=2
      IF ((V6.GE.0.).AND.(V7.GE.0.).AND.(V8.GE.0.)) IPSW=1
      RETURN
      END
```

Figure C-2 (Continued)

```
      SUBROUTINE BOUND(B1,B2,B3,FO,FI,FII,FIII,
     1    ETA ,BI1,BI2,BI3,IBSW)
C THIS SUBROUTINE SETS THE BOUNDARY CONDITIONS AT THREE
C SURFACES OF A FINITE CYLINDER INDEPENDENT OF EACH OTHER.
C PROVISIN IS MADE TO ACCOUNT FOR LINEARLY VARYING HEAT
C TRANSFER COEFFICIENT AT THE BEGINNING AND END OF HEAT
C TRANSFER INTERVAL
         B1=BI1
         B2=BI2
         B3=BI3
         IBSW=2
      IF (FO.GE.FI) GO TO 10
         B1=BI1*FO/FI
         B2=BI2*FO/FI
         B3=BI3*FO/FI
         IBSW=1
      RETURN
   10 IF (FO.LT.FII) GO TO 20
      IF(FO.GT.FIII) GO TO 40
         B1=BI1*(FIII-FO)/(FIII-FII)
         B2=BI2*(FIII-FO)/(FIII-FII)
         B3=BI3*(FIII-FO)/(FIII-FII)
         IBSW=3
     RETURN
  40    B1=0.
        B2=0.
        B3=0.
        IBSW=4
  20 CONTINUE
     RETURN
     END
```

Figure C-2 (Continued)

```
      SUBROUTINE FINITE (N,M,AMR,AMZ,ETA,TH,V0,V1,
     1 V2,V3,V4,V5,V6,V7,V8,V,W)
      DIMENSION TH(10,10),TTH(10,10),V(10),W(10)
         NP=N+1
         MP=M+1
      TTH(NP,1)=TH(NP,1)*V7+TH(N,1)*2.*AMR
     6   +TH(NP,2)*2.*AMZ+V1+V0
      TTH(NP,MP)=TH(NP,MP)*V8+TH(NP,M)*2.*AMZ
     7   +TH(N,MP)*2.*AMR+V2+V0
      TTH(1,1)=TH(2,1)*2.*AMR+TH(1,1)*V4
     8       +TH(1,2)*2.*AMZ+V1
      TTH(1,MP)=TH(2,MP)*2.*AMR+TH(1,MP)*V5
     9    +TH(1,M)*2.* AMZ+V2
      DO 30 I=2,N
      TTH(I,1)=TH(I+1,1)*V(I)+TH(I,1)*V4
     3   +TH(I-1,1)*W(I)+TH(I,2)*2.*AMZ+V1
       TTH(I,MP)=TH(I+1,MP)*V(I)+TH(I,MP)*V5
     4    +TH(I-1,MP)*W(I)+TH(I,M)*2.*AMZ+V2
   30 CONTINUE
      DO 40J=2,M
      TTH(1,J)=TH(2,J)*2.*AMR+TH(1,J)*V3
     2    +TH(1,J+1)*AMZ+TH(1,J-1)*AMZ+(TH(2,J)-TH(1,J))*2.*AMR
      TTH(NP,J)=TH(NP,J)*V6+TH(N,J)*2.*AMR
     5  .+TH(NP,J+1)*AMZ+TH(NP,J-1)*AMZ+V0
   40 CONTINUE
      DO 50 I=2,N
      DO 50J=2,M
         TTH(I,J)=TH(I+1,J)*V(I)+TH(I,J)*V3
     1       +TH(I-1,J)*W(I)+TH(I,J+1)*AMZ
     1       +TH(I,J-1)*AMZ
   50 CONTINUE
      DO 60 I=1,NP
      DO60J=1,MP
         TH(I,J)=TTH(I,J)
   60 CONTINUE
      RETURN
      END
```

Figure C-2 (Concluded)

CASE NO. 64

FO	BI1	BI2	BI3	THBAR	ETA
.001	.600	.600	2.000	.009	.600

	1	2	3	4	5	6	7
1	.040	.040	.040	.040	.040	.040	.066
2	.000	.000	.000	.000	.000	.000	.026
3	.000	.000	.000	.000	.000	.000	.026
4	.000	.000	.000	.000	.000	.000	.026
5	.000	.000	.000	.000	.000	.000	.026
6	.000	.000	.000	.000	.000	.000	.026
7	.040	.040	.040	.040	.040	.040	.066

FO	BI1	BI2	BI3	THBAR	ETA
.005	.600	.600	2.000	.046	.600

	1	2	3	4	5	6	7
1	.130	.130	.130	.130	.130	.138	.225
2	.026	.026	.026	.026	.026	.034	.131
3	.003	.003	.003	.003	.003	.012	.110
4	.000	.000	.000	.000	.001	.009	.108
5	.003	.003	.003	.003	.003	.012	.110
6	.026	.026	.026	.026	.026	.034	.131
7	.130	.130	.130	.130	.130	.138	.225

FO	BI1	BI2	BI3	THBAR	ETA
.010	.600	.600	2.000	.089	.600

	1	2	3	4	5	6	7
1	.186	.186	.186	.186	.189	.211	.331
2	.065	.065	.065	.065	.068	.094	.231
3	.017	.017	.017	.017	.020	.047	.191
4	.006	.006	.006	.006	.009	.036	.182
5	.017	.017	.017	.017	.020	.047	.191
6	.065	.065	.065	.065	.068	.094	.231
7	.186	.186	.186	.186	.189	.211	.331

FO	BI1	BI2	BI3	THBAR	ETA
.050	.600	.600	2.000	.355	.600

	1	2	3	4	5	6	7
1	.377	.379	.384	.400	.436	.506	.618
2	.270	.272	.278	.296	.339	.421	.552
3	.204	.205	.212	.232	.278	.368	.512
4	.181	.183	.190	.210	.258	.351	.498
5	.204	.205	.212	.232	.278	.368	.512
6	.270	.272	.278	.296	.339	.421	.552
7	.377	.379	.384	.400	.436	.506	.618

Figure C-3 Output Format

	.400	.600	.600	2.000	.963	.600	
	1	2	3	4	5	6	7
1	.957	.958	.960	.964	.969	.974	.981
2	.950	.951	.953	.958	.963	.970	.977
3	.945	.946	.949	.954	.960	.967	.975
4	.944	.945	.948	.952	.959	.966	.974
5	.945	.946	.949	.954	.960	.967	.975
6	.950	.951	.953	.958	.963	.970	.977
7	.957	.958	.960	.964	.969	.974	.981
	FO	BI1	BI2	BI3	THBAR	ETA	
	.600	.600	.600	2.000	.993	.600	
	1	2	3	4	5	6	7
1	.992	.992	.992	.993	.994	.995	.996
2	.990	.990	.991	.992	.993	.994	.996
3	.989	.989	.990	.991	.992	.994	.995
4	.989	.989	.990	.991	.992	.993	.995
5	.989	.989	.990	.991	.992	.994	.995
6	.990	.990	.991	.992	.993	.994	.996
7	.992	.992	.992	.993	.994	.995	.996
	FO	BI1	BI2	BI3	THBAR	ETA	
	.100	.600	.600	2.000	.574	.600	
	1	2	3	4	5	6	7
1	.546	.552	.566	.591	.633	.691	.764
2	.469	.475	.491	.521	.569	.637	.724
3	.421	.427	.444	.477	.530	.604	.699
4	.405	.410	.428	.462	.516	.593	.690
5	.421	.427	.444	.477	.530	.604	.699
6	.469	.475	.491	.521	.569	.637	.724
7	.546	.552	.566	.591	.633	.691	.764
	FO	BI1	BI2	BI3	THBAR	ETA	
	.200	.600	.600	2.000	.812	.600	
	1	2	3	4	5	6	7
1	.785	.790	.800	.817	.840	.868	.900
2	.749	.753	.766	.785	.812	.845	.883
3	.726	.731	.744	.766	.795	.831	.872
4	.719	.723	.737	.759	.789	.826	.869
5	.726	.731	.744	.766	.795	.831	.872
6	.749	.753	.766	.785	.812	.845	.883
7	.785	.790	.800	.817	.840	.868	.900
	FO	BI1	BI2	BI3	THBAR	ETA	

Figure C-3 (Concluded)

APPENDIX D
PRODUCT SOLUTION METHOD

Principle

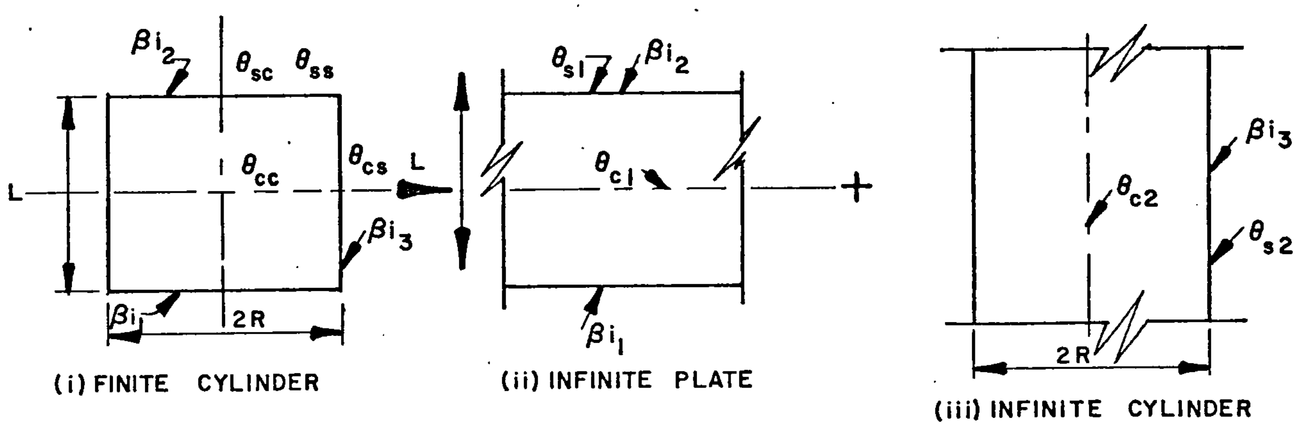

Figure D-1 Representation of a Product Solution

The boundary conditions and terminology for temperature distribution are defined in Figure D-1.

At time t let Fo, Fo_1 and Fo_2 be the dimensionless times for the finite cylinder, the infinite plate and the infinite cylinder respectively, then

$$Fo = \frac{\alpha t}{R^2}, \tag{D-1}$$

$$Fo_1 = \frac{\alpha t}{(L/2)^2} = \frac{4\alpha t}{R^2\eta^2} = \frac{4}{\eta^2}\, Fo, \tag{D-2}$$

$$Fo_2 = Fo \tag{D-3}$$

If h_1, h_2 and h_3 are the convection heat transfer coefficients at the bottom, top and lateral surfaces of a finite can, then

$$Bi_1 = \frac{h_1 L}{2k} = \frac{h_1 R}{k}\,\frac{\eta}{2} = \frac{\eta h_1 R}{2k} \qquad \text{(D-4)}$$

$$Bi_2 = \frac{\eta h_2 R}{2k} \qquad \text{(D-5)}$$

$$Bi_3 = \frac{h_3 R}{k} \qquad \text{(D-6)}$$

The product solution method can be mathematically expressed as

$$(1-\Theta) = (1-\Theta_1)\cdot(1-\Theta_2) \qquad \text{(D-7)}$$

where

Θ= temperature in the finite cylinder at time Fo,

Θ_1= temperature in the infinite plate at time Fo_1,

Θ_2= temperature in the infinite cylinder at time Fo_2.

In the special cases,

$$(1-\Theta cc) = (1-\Theta c_1)\cdot(1-\Theta c_2) \qquad \text{(D-8)}$$

$$(1-\Theta cs) = (1-\Theta c_1)\cdot(1-\Theta s_2) \qquad \text{(D-9)}$$

$$(1-\Theta sc) = (1-\Theta s_1)\cdot(1-\Theta c_2) \qquad \text{(D-10)}$$

$$(1-\Theta ss) = (1-\Theta s_1)\cdot(1-\Theta s_2) \qquad \text{(D-11)}$$

where Θc_1, Θc_2, Θs_1, Θs_2, Θcc, Θcs, Θsc and Θss are defined in figure D-1.

Applications in two Specific Cases

Exact solutions are available for an infinite plate and an infinite cylinder, reference [6]. The solutions are utilized in deriving exact solutions at specific points of a finite cylinder in two separate cases. The summarized results for these cases are shown in Tables D-1 and D-2.

Table D-1. Response Temperatures for a Finite Cylinder (L/R=2) with $Bi_1=Bi_2=Bi_3=2$

Time	Response Temperature							
	Infinite Plate		Infinite Cylinder		Product Solution Temperature			
Fo	θc_1	θs_1	θc_2	θs_2	θcc	θcs	θsc	θss
.001		.065		.075		.075	.065	.14
.005		.14		.14		.14	.14	.26
.01		.19		.19		.19	.19	.34
.05		.35		.39		.39	.35	.60
.1	.01	.44	.04	.50	.04	.50	.44	.72
.2	.08	.52	.21	.63	.27	.66	.62	.82
.4	.26	.65	.52	.79	.64	.84	.83	.93
.6	.42	.73	.70	.91	.83	.95	.92	.98
1.0	.63	.82	.90	.95	.96	.98	.98	.99

Table D-2 Response Temperatures for a Finite Cylinder with L/R =1, $Bi_1=Bi_2=1$, $Bi_3=2$

Infinite Plate			Infinite Cylinder			Finite Cylinder				
							Product Solutions			
Fo_1	$\theta c1$	$\theta s1$	Fo2	$\theta c2$	$\theta s2$	Fo	θcc	θcs	θsc	θss
.004		.03	.001		.06	.001		.03	.06	.09
.020		.12	.005		.12	.005		.12	.12	.22
.04		.18	.01		.19	.01		.19	.18	.34
.20	.05	.34	.05		.39	.05	.05	.42	.34	.60
.4	.18	.46	.1	.04	.50	.1	.21	.59	.48	.73
.8	.38	.60	.2	.21	.63	.2	.51	.77	.68	.85
1.6	.64	.78	.4	.52	.79	.4	.83	.92	.89	.95
2.4	.81	.86	.6	.70	.91	.6	.94	.98	.96	.99
4.0	.94	.97	1.0	.90	.95	1.0	.99	.999	.999	.999
8.0	.998	.999	2.0	.99	.999	2.0	.999	.999	.999	.999

REFERENCES

(1) Carslaw H. S. and Jaeger J. C. Conduction of Heat in Solids. 2nd Ed; London: Oxford University Press. 1959.

(2) Cheng Y. T. E., Cox J. E. and Witte L. C. Characterization of Heat Transfer in Nutrient Materials. Monthly Progress Report submitted to NASA under Contract No. NAS-9- 11676. University of Houston. 1975

(3) Cox J. E., Bannerot R. B., Chen C. K., and Witte L. C. Characterization of Heat Transfer in Nutrient Materials. Monthly Progress Report submitted to NASA under Contract No. NAS-9-11676. University of Houston. 1973.

(4) Fairchild Republic Division, Final Report: Space Shuttle/Food System Study. 1975.

(5) Hildebrandt F. B. Advanced Calculus for Applications. New Jersey: Prentice Hall. 1962.

(6) Luikov A. V. Analytical Heat Diffusion Theory. Edited by James P. Hartnett. New York: Academic Press. 1968.

(7) Mathias, M. R. "A Study of the Effects of Cyclic (On-off) Heat Fluxes on Canned Food Heating Times During Skylab Space Flights," M.S. Thesis, University of Houston, Department of Mechanical Engineering, August 1972.

(8) Olcer N. Y. "General Solution to a Class of Heat Flow Problems in a Finite Circular Cylinder," Brit. J. Appl. Physics, Vol. 18, pp. 89-105, 1967.

(9) Reiser M. J. and Appl. F. J. "A Numerical Method for Heat Conduction Problems," Journal of Heat Transfer, pp. 307-312, August 1974.

(10) Rohsenow W. M. and Hartnett J. P. ed. Handbook of Heat Transfer, New York: McGraw-Hill, "Method of Obtaining Approximate Solutions" by P. Razelos, 1973.

(11) Schneider P. J. Temperature Response Charts, New York: John Wiley, 1963.